1980

Reduction of capacitor switching transients by controlled closing

John Herman Brunke
Portland State University

AN ABSTRACT OF THE THESIS OF John Herman Brunke for the Master of Science in Applied Science presented June 3, 1980.

Title: Reduction of Capacitor Switching Transients by Controlled Closing

APPROVED BY THE MEMBERS OF THE THESIS COMMITTEE:

[redacted]

Jack C. Riley, Chairman

[redacted]

Nan-Teh Hsu

[redacted]

J. Michael Heneghan

[redacted]

George G. Lendaris

This thesis presents the theory, analysis, testing and implementation of a scheme to reduce shunt compensation capacitor switching transients. The described method is switch the capacitors very near the instant when the bus voltage is at a power frequency zero. This was accomplished with a vacuum breaker on a 230 kV shunt capacitor bank.

REDUCTION OF CAPACITOR SWITCHING TRANSIENTS BY CONTROLLED CLOSING

by

JOHN HERMAN BRUNKE

A thesis submitted in partial fulfillment of the

requirements for the degree of

MASTER OF SCIENCE
in
APPLIED SCIENCE

Portland State University

1980

TO THE OFFICE OF GRADUATE STUDIES AND RESEARCH:

The members of the Committee approve the thesis of John Herman Brunke presented June 3, 1980.

[redacted]

Jack C. Riley, Chairman

[redacted]

Nan-Teh Hsu

[redacted]

J Michael Heneghan

[redacted]

George G Lendaris

APPROVED:

[redacted]

Ralph D. Greiling, Acting Head
Electrical-Electronics Engineering

[redacted]

Stanley E. Rauch
Dean of Graduate Studies and Research

Acknowledgments

I would like to thank the Bonneville Power Administration who financed this project. In addition, I would like to thank Guenter G. Schockelt, Howard King, Eldon Rogers, and the many others who participated in this project.

TABLE OF CONTENTS

LIST OF TABLES

LIST OF FIGURES

LIST OF FIGURES (Continued)

LIST OF FIGURES (Continued)

LIST OF FIGURES (Continued)

LIST OF FIGURES (Continued)

LIST OF FIGURES (Continued)

CHAPTER I

INTRODUCTION

When a shunt capacitor bank is connected to a high voltage power system during the high voltage part of the voltage cycle a current surge subjects electrical insulation and control circuitry to excessive stresses. These stresses can be minimized by making the connection when the voltage is near its zero-crossover value.

This thesis reports the design, performance and application of a capacitor bank switching system which is constrained to operate only when the 230,000 volt bus voltage is near its zero-crossover value.

Capacitor switching transients have been identified as the cause of insulation failures of high voltage equipment and of the control circuitry within the substation. Capacitor banks are used for power factor correction. The banks must be energized and de-energized as the load fluctuates. Since the load changes many times during the day, the capacitor switching transients are one of the most frequent stresses applied to the system. As system voltages increase, both economical and physical constraints demand that surges be limited to lower levels.

Recent successes in limiting switching surges on 500-kV systems with power circuit breakers equipped with devices to control their instant of closing(1) led to interest in applying the same technique to other switching surge limiting problems.

The application of synchronous switching to reduce shunt capacitor energization transients had already been accomplished at low voltages (600 volts) where solid-state switching devices can be used(2). At the voltage levels on power transmission systems a mechanical switching

device is required. This thesis reports on the application of synchronous switching to control inrush transients when switching shunt capacitors on a 230,000 volt power transmission system(3).

CHAPTER II

CAPACITOR SWITCHING TRANSIENTS

A study was undertaken to find the parameters which would be required of the switching device. By mathemetically analyzing a circuit model the expected system stesses can be predicted and system specifications can be postulated.

The first step in analyzing capacitor switching transients is the development of a sufficiently accurate model. Figure 1 represents the equivalent circuit of a single phase of a grounded wye shunt capacitor bank.

The worst case switching transient for energizing a shunt capacitor bank occurs when the switch is closed at maximum voltage. The physical limitations of existing switches increase the probability of this worst case condition. The switches close slowly relative to the 60 hertz voltage fluctuation. Contact breakdown due to high voltage stress causes the circuit to be connected when maximum voltage occurs even though physical closure has not yet occurred.

The devices used to switch shunt capacitor banks include power circuit breakers and load break switches. Although the close signals supplied to these devices are random in time, the voltage phase angle at the instant of circuit energization has a nonuniform statistical distribution(4). Mechanical contact closure has a uniform distribution, but electrical breakdown of the insulating medium can occur

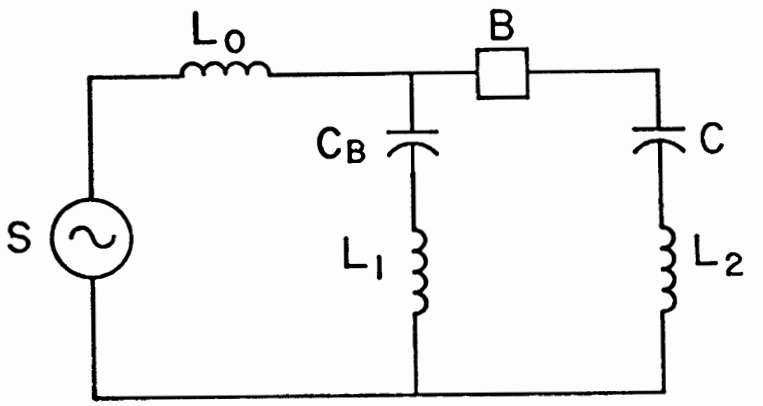

Figure 1 The equivalent circuit of a single phase of a grounded wye shunt capacitor bank. The parameters represent:

C The capacitance of the capacitor bank to be energized.

L_o The inductance of the source.

C_B The capacitance of the bus to ground. This parameter can vary greatly depending upon the circuit configuration.

L_1 The inductance of the capacitor bus and ground return.

L_2 The inductance of a second capacitor bus and ground return. This parameter is not included in some circuit configurations.

B This is the switching device that energizes the capacitor bank.

prior to mechanical contact closure (prestrike). The degree to which this occurs depends primarily upon: (1) the dielectric strength of the insulating medium, (2) contact velocity, and (3) the electric field gradient due to contact shape. The performance of the load break switch with its relatively slow moving contacts, insulated by atmospheric pressure air, precludes energization at any point other than very near crest voltage. It will be necessary to explore this in greater depth later.

Since it is the common practice and allow capacitors to fully discharge through their internal discharge resistor prior to reenergizing them, it can be assumed that there is no charge upon them when they are energized.

We must now divide capacitor switching transients into two separate cases, "single bank" and "back to back", each with its own characteristic transients. In the "single bank" case the bus capacitance is very small (nanofarads) compared to the capacitance of the capacitor bank (microfarads) to be switched on to the bus. In the "back to back" case the magnitudes of the bus and capacitor bank capacitances are nearly equal (microfarads). The bus capacitance is this high because another capacitor bank (or more than one) has been previously energized and is already connected to the bus, hence the name "back to back."

Previous solutions were usually made using equivalent circuits similar to that shown in figure 1 and a superposition of the transient and steady state results (5, 6, 7, 8, 9, 10). This method allows a understanding of the nature of the transients and the results this method predicts have been verified by field tests. To give a more

accurate solution, an electromagnetic transients computer program that was developed at BPA was used(11). It provides capabilities that greatly exceed those needed for a solution of this problem. An even more complex model could have been used incorporating factors such as skin effect, nonlinear damping and a distributed parameter bus. However, such factors have a minor effect(12). This conclusion was substantiated by sample calculations and tests.

The "single bank" energization is known to frequently produce a severe voltage transient. Figure 2 shows the equivalent circuit that will be used for the explanation of the transient. The bus inductance and capacitance are represented as well as the source impedance and bank capacitance.

The high frequency transient is dominated by the current path shown in Figure 3. The transient current and resulting bus voltage can be determined using the Laplace transform technique as follows:

$$I_H(s) = \frac{V}{sL_2 + 1/C + 1/CB} \tag{1}$$

$$\text{Letting} \quad w_H^2 = \frac{C+C_B}{CC_BL_2} \tag{2}$$

$$I_H(s) = \frac{V/L_2}{s^2 + w_H^2} \tag{3}$$

$$i_H(t) = (V/wL_2)\sin wt \tag{4}$$

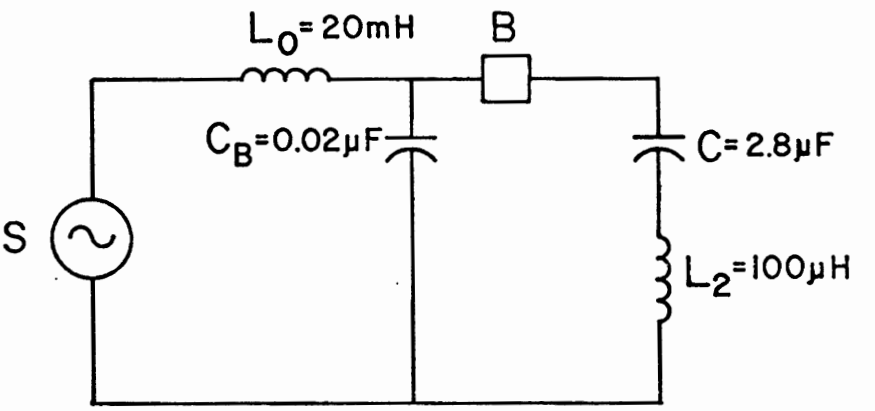

Figure 2 The equivalent circuit for the "single bank" case.

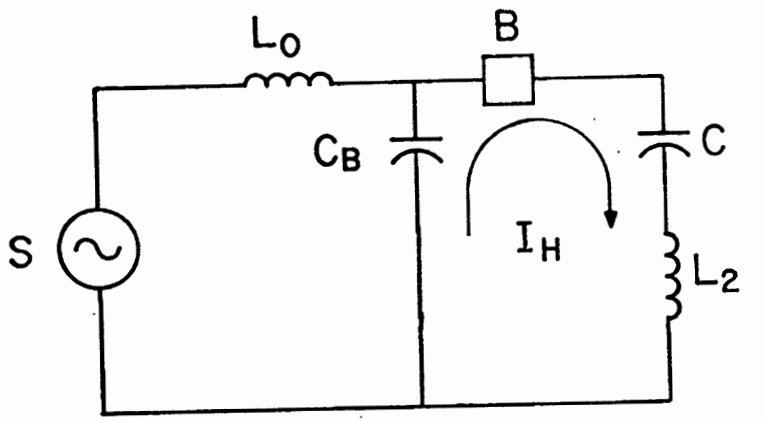

Figure 3 The equivalent circuit for the "single bank" case showing the path of the high frequency transient current.

The bus voltage V_B can also be found:

$$V_B(s) = V[1/s - I(s)(1/sC_B)] \tag{5}$$

$$v_B(t) = V[1 - C/(C-C_B)(1-\cos wt)] \tag{6}$$

We can see that the magnitude of the transient depends upon the magnitude of the voltage at the instant of energization. If we insert numerical values from Figure 2 into equation (6), we find that the bus voltage dips to 1 percent of its initial value and does this in 2.2 us. The ringing frequency of this portion of the transient is slightly over 100 kHz.

We can also calculate the rate of change of bus voltage:

$$\frac{dv_B(t)}{dt} = (wC)/(C+C_B)\sin wt \tag{7}$$

This solution will yield a slower rate of change of bus voltage than the actual case as we have lumped the bus capacitance at the point where we are making the measurement. Inserting numerical values still yields a rate of change of bus voltage of 140 kV/us. In the calculations for the "back to back" case the other extreme will be examined.

The low frequency position of the oscillation that occurs when single banks are energized can be investigated using the circuit in figure 4, which can be analyzed as follows:

$$I_L(s) = \frac{V/s}{sL_O + 1/sC} \tag{8}$$

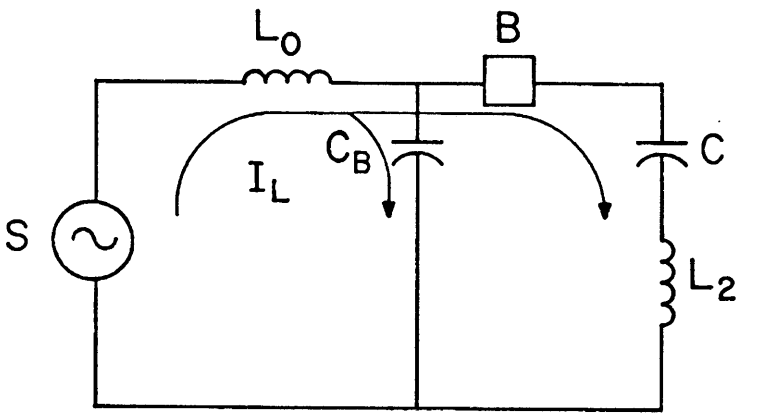

Figure 4 The equivalent circuit for the "single bank" case showing the path of the low frequency transient current.

Letting $w^2 = 1/L_0C$ (9)

$$I_L(s) = (V/L_0)[w/(s^{2+}w^2)] \quad (10)$$

$$i_L(t) = [V\sqrt{(L_0/C)}]\sin wt \quad (11)$$

The estimated parameters yield peak currents of over 2,000 amperes at frequencies near 1 kHz.

The superimposed effect of these transients and the steady state performance were obtained by computer analysis. The result is plotted in Figure 5. Linear resistance damping was included in the computer analysis.

Computer studies were run for contact closure at different phase angles of the bus voltage. See Appendix I.

Both the high frequency and low frequency models demonstrate that the transient magnitudes are proportional to the voltage magnitude at the instant of energization. This suggests that performance might be improved by minimizing the voltage magnitude at the instant of energization.

The back to back energization is known to frequently cause a severe current transient. Figure 6 shows the equivalent circuit that will be used to analyze the "back to back" transient. The parameters are the same as for the single bank case with the exception of a greatly increased magnitude of the bus capacitance, and the addition of L_2 which is assumed to be equal to L_1.

We can again solve for the high frequency transient current (Figure 7):

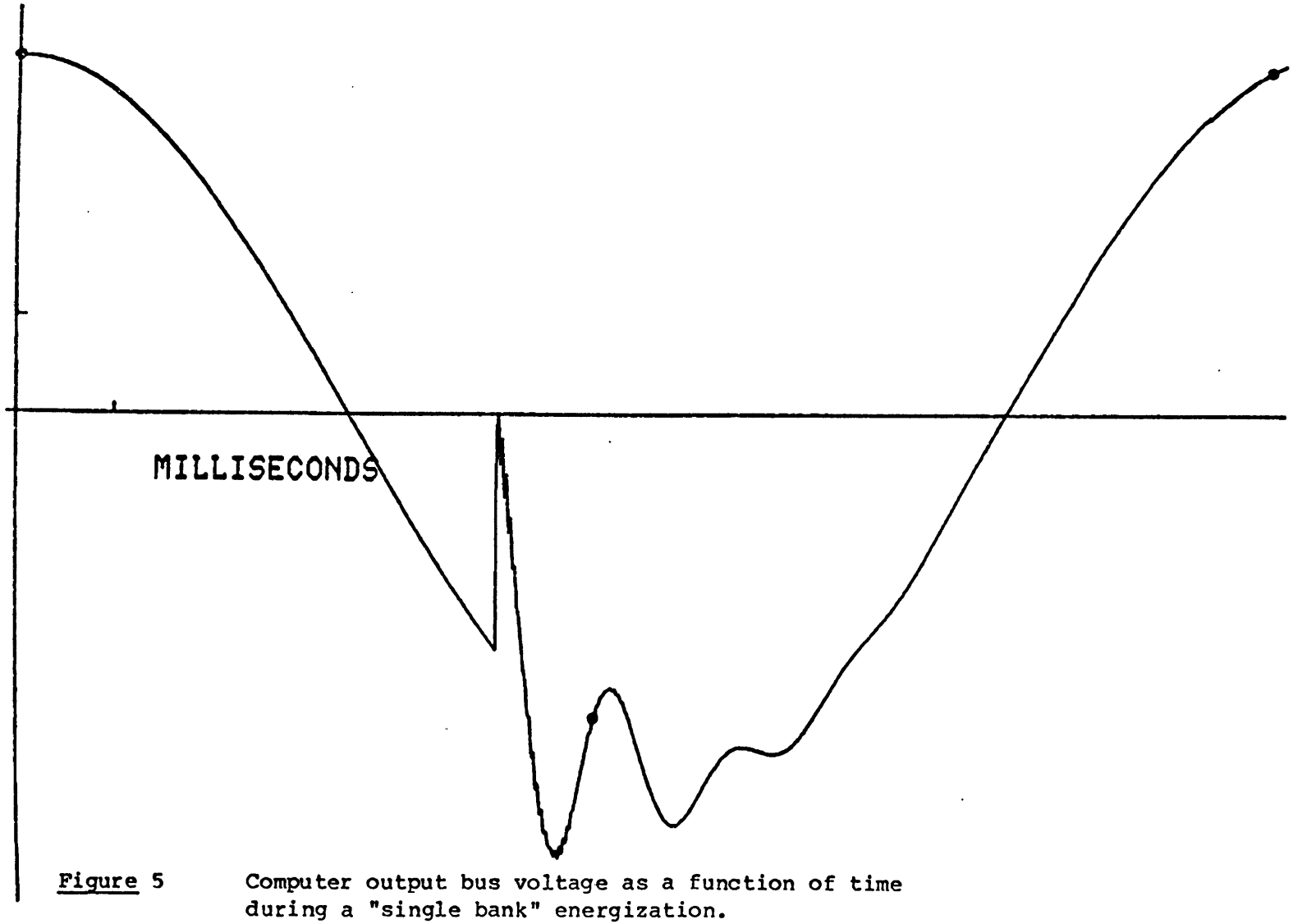

Figure 5 Computer output bus voltage as a function of time during a "single bank" energization.

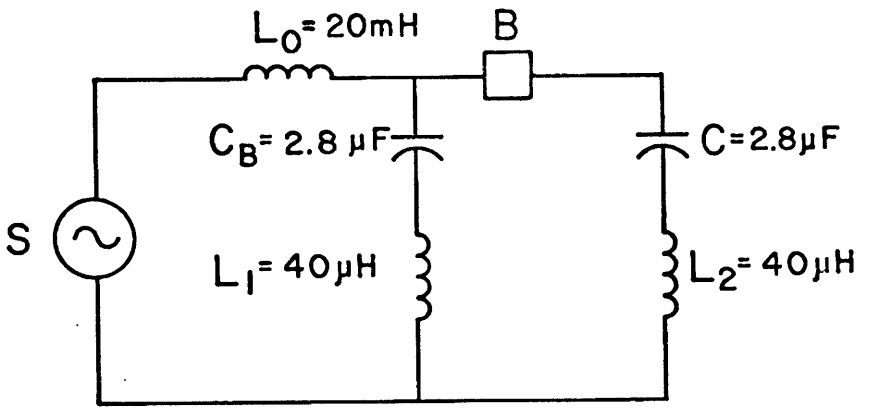

Figure 6 The equivalent circuit for the "back to back" case.

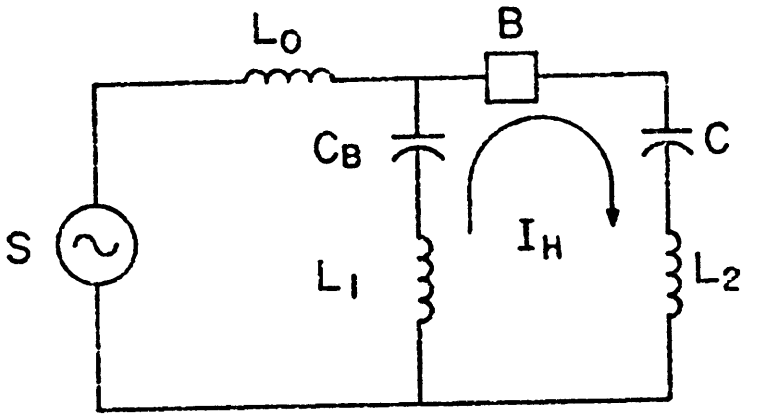

Figure 7 The equivalent circuit for the "back to back" case showing the high frequency current path.

$$I_H(s) = \frac{V/S}{(L_1+{}_2L)s + 1/sC_B - 1/sC} \quad (12)$$

$$w^2 = (C_B+C)/[(L_1+L_2)C_BC] \quad (13)$$

$$I_H(s) = \frac{V}{(L_1+L_2)\ (s^2+w^2)} \quad (14)$$

$$i_H(t) = (V/[(L_1+L_2)w])\sin wt \quad (15)$$

And the bus voltage becomes:

$$V_b(s) = (V/s) - I(s)(L_2s + 1/sC_B) \quad (16)$$

$$v_B(t) = V(1 - [L_2/(L_1+L_2)])\cos wt + [C_B/(C+C_B)](1-\cos wt) \quad (17)$$

Now the initial voltage dip is much steeper (instantaneous in the model). This is due to the lack of capacitance at the point of voltage measurement. A distributed parameter model is necessary to more nearly predict the true rate of fall of voltage. For the back to back case the voltage dips to 50 percent of its initial value when bus and capacitor bank capacitances are equal.

The numerical values yield peak currents near 25,000 amperes at frequencies near 10 kHz. It can be noted that the solution of Equation (17) that it is very sensitive to the magnitudes of L_1 and L_2. This inductance represents approximately 200 feet of 4-inch bus.

The low frequency transient is the same as that for the single bank case except for the parallel capacitance of the two banks. Again a computer solution with damping included is shown in Figures 26 through 45 in Appendix I.

As the previous analysis was for only one phase of a three phase system, it should also be noted that for both the "single bank" and "back-to-back" cases variations exist between the first phase and the last phase to close(13). This is due to the effects of the other phases already connected to the common neutral. The effects of these previously connected phases do affect the transients in the late phase by up to 13 percent. This is not significant to this study. Figure 8 illustrates differences between the equivalent circuits, depending upon closing sequence.

Results of the computer studies for both cases, as shown in Appendix I, indicate that the peak inrush current is proportional to the magnitude of the voltage at the instant of energization. The magnitude of the voltage dip and the overshoot are also directly proportional to the magnitude of the voltage at the instant of energization for each case. These results are expressed in Figures 9 and 10. The peak current vs. time follows the sinusodial shape of the voltage wave. The relation between, in this case peak inrush current, and timing deviation from voltage zero is a quarter cycle of the 60 Hz. wave. The model, therefore, indicates that energization close to zero volts will significantly reduce inrush current magnitude.

When a single bank is energized the bus voltage experiences a very sudden drop which intitiates a ringing that results in an overvoltage transient. These unwanted voltage excursions are transmitted along the

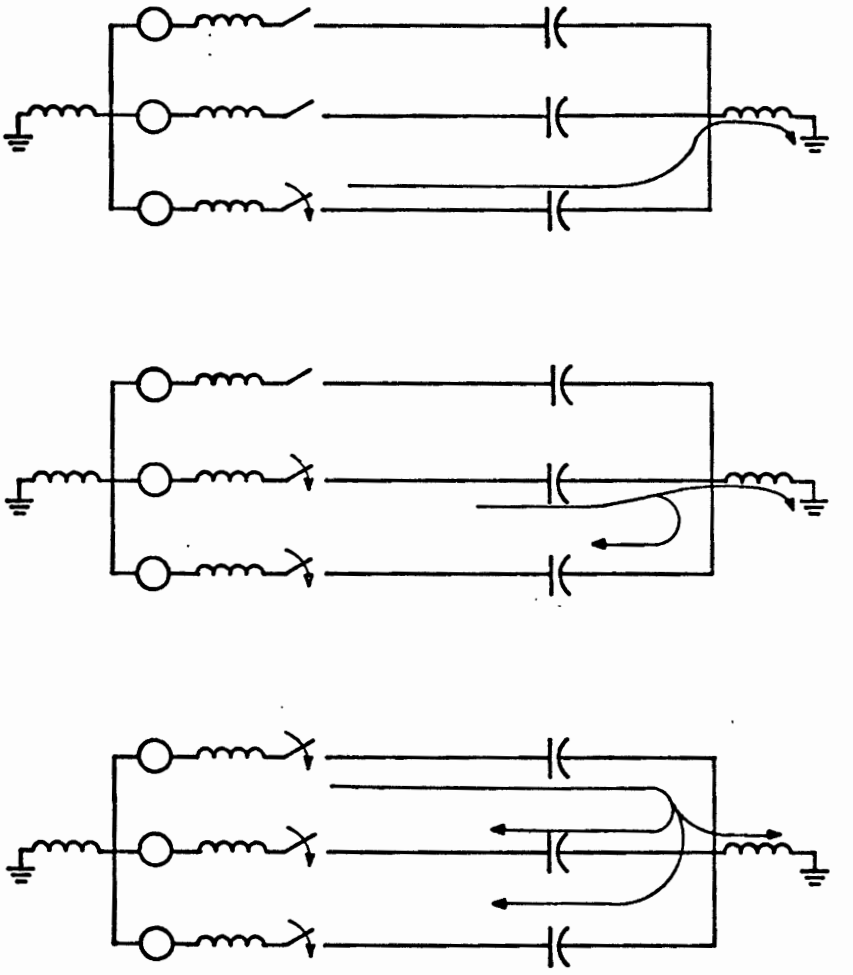

Figure 8 Simplified diagrams of a three-phase capacitor bank showing current paths which result in difference parameters for each phase, dependent upon the closing sequence.

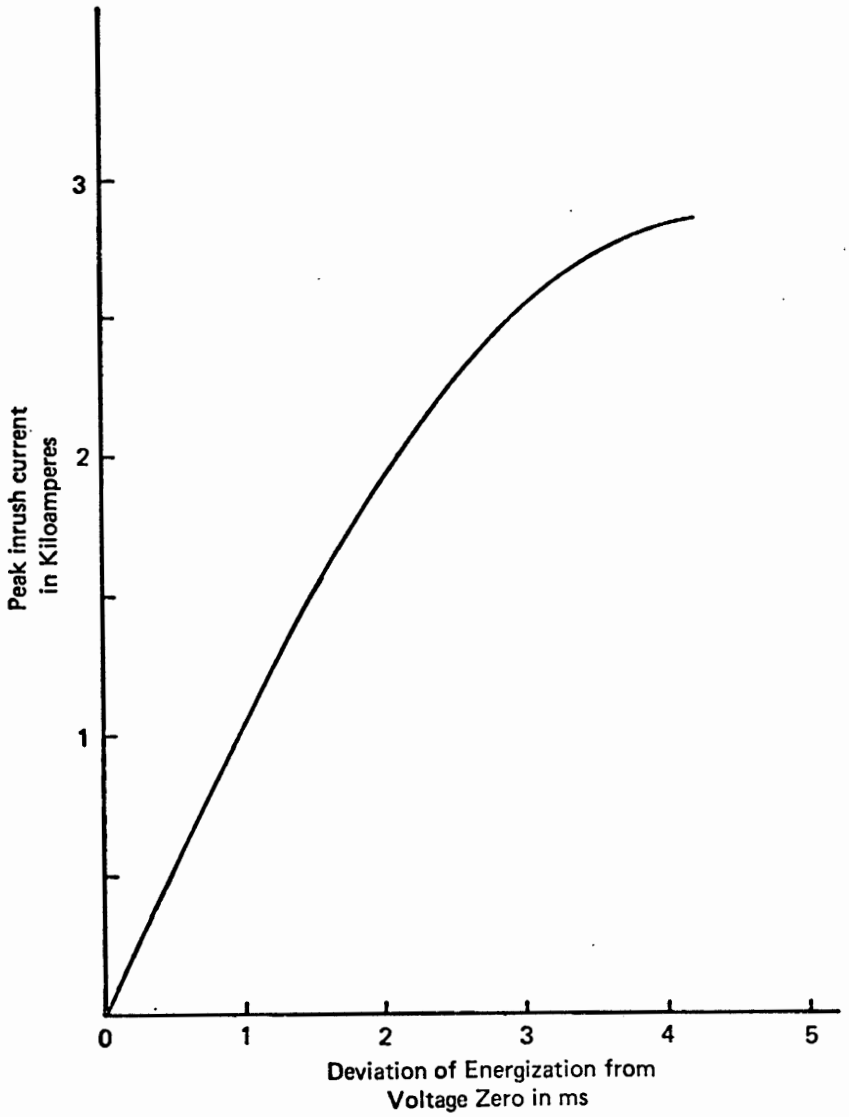

Figure 9 The calculated peak magnitudes of inrush current as a function of timing deviation from voltage zero for the "single bank" case.

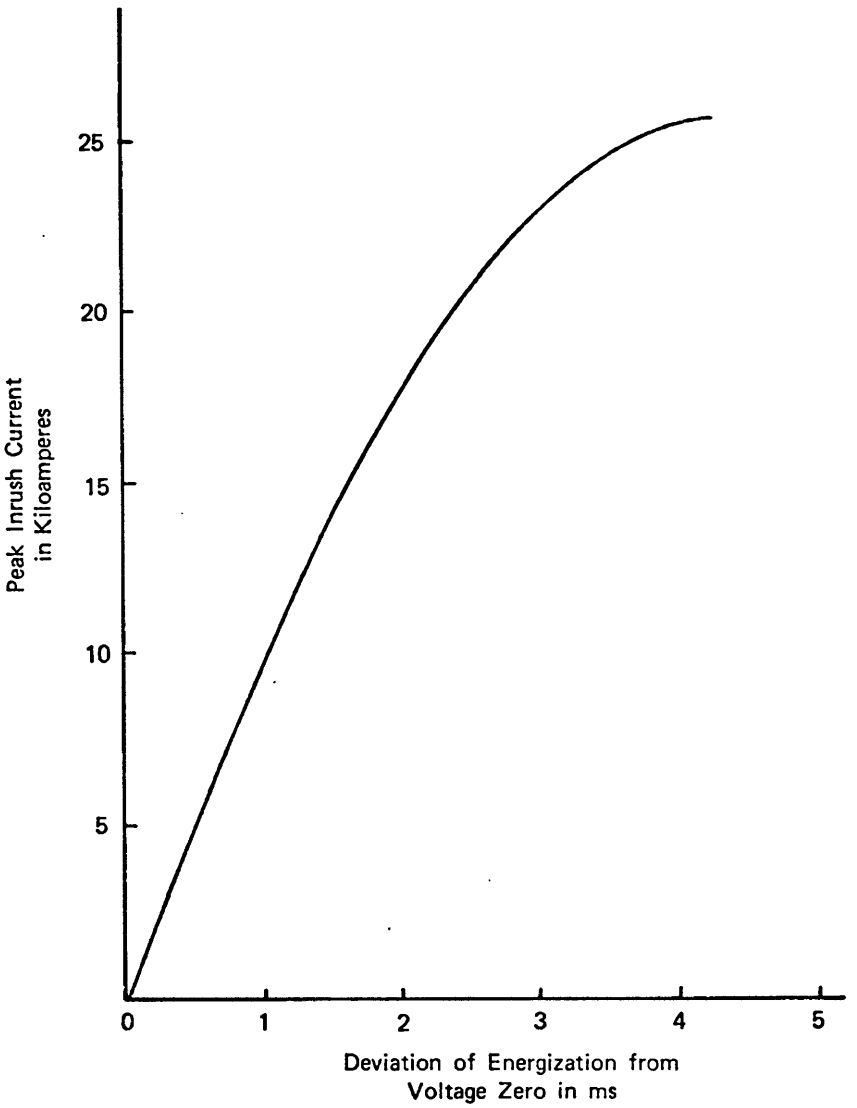

Figure 10 The calculated peak magnitudes of inrush current as a function of timing deviation from voltage zero for the "back to back" case.

busses to all adjoining lines. The intitial voltage drop is below the crest voltage and will not exhibit any corona discharge which could help to reduce its effects. Surge arrestors offer no help because they are designed to protect against voltage rises. A voltage wave with such a high dV/dt can severely stress transformer windings. The bus voltage overshoots then, which can cause insulation failures if equipment is not protected.

The high magnitude currents that occur during back to back switching cause an entirely different set of problems, even causing a ground potential rise in portions of the station ground mat. This can result in such things as flashover of nearby fences to ground, flashovers of control circuits, station service, and other wiring in the substation. Dangerously high step potentials (potentials between points on the ground, specifically, between a man's feet) and touch potentials (potentials between ground and nearby grounded objects that a man's hands might touch) can also result. Although areas where these ground potentials are highest are usually fenced, potentials in unfenced areas may trigger other accidents. Induced currents in station wiring can cause insulation breakdowns and flashovers(14).

In addition to special grounding and shielding systems to reduce the effects of inrush current transients, there are methods to reduce the magnitude of the transients themselves. These include:

1. Preinsertion resistors. A resistor that is inserted as the first element to complete the circuit, it is bypassed in approximately 1/6 of a second. Values usually range from 20 ohms to 85 ohms depending on application. A second transient occurs when the resistor is bypassed. An picture of

this device is shown in Figure 11. The resistor reduces the magnitude of the initial step and provides rapid damping.

2. Current limiting reactors. An inductor that is permanently in the circuit. It increases the bus inductance, limiting the current and the steepness of the voltage dip. Values usually are near 1.5 mH.

3. Controlled closing. A method to energize the circuit while the voltage across the capacitor is near zero. This has been done successfully at low voltages using solid state switching devices(2). The subject of this thesis is the development of a practical system to accomplish this controlled closing for very high voltage circuits.

The results of the computer studies indicate that capacitor energization within $\pm$ 0.25 ms of voltage zero would be required to provide the same reduction in inrush current magnitude as preinsertion resistors(15). This type of accuracy was not thought reasonable. Studies indicate that a timing accuracy of $\pm$ 1.0 ms would provide: (1) a 70 percent reduction in inrush current from the no resistor or random case, (2) would prevent any bus overvoltage, and (3) would reduce the magnitude of the voltage dip, but not its slope. The accuracy of $\pm$ 1.0 ms was selected as the timing accuracy goal for the switching device because it was thought to be obtainable and adequate.

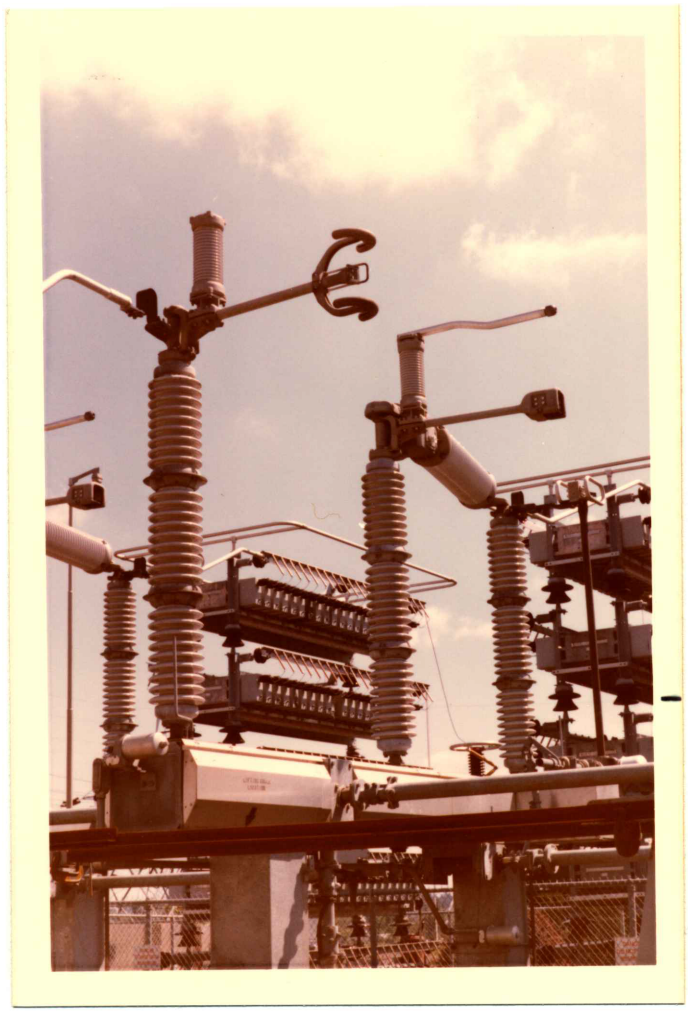

Figure 11 A load break switch with preinsertion resistors. The arcing horn has been removed from the resistor on the left for the field test. The capacitors can be seen in the background.

CHAPTER III

THE SWITCHING DEVICE

The performance requirements for a switching device to accomplish voltage zero switching are very special.

In order to energize a circuit at voltage zero the switching device must exhibit a rate of change of dielectric strength (breakdown voltage) across its closing contacts which is greater than the maximum rate of change of the system voltage. Figure 12 illustrates the 60 Hz wave and required rate of change of dielectric strength to permit energization at voltage zero. On the 230 kV system the maximum rate of change of voltage is:

$$\frac{dV}{dt} = \frac{d}{dt} \; 198 \times 10^3 \sin 377t$$

$$= 75 \times 10^6 \cos 377t$$

$$\frac{dV}{dt} \text{ max} = 75 \times 10^6 \text{ volts/second}$$

That is, the maximum rate of change of voltage is 75 million volts per second. If we assume an approximate atmospheric pressure air breakdown of 100 kV per foot, we can calculate the necessary contact velocity of air insulated contacts to be 750 feet per second. This is not a practical contact velocity so an insulating medium other than air is indicated.

A vacuum breaker was a likely candidate for this application. Vacuum exhibits a very high rate of change of dielectric strength. Average breakdown voltage for vacuum contacts is 1 MV/cm or

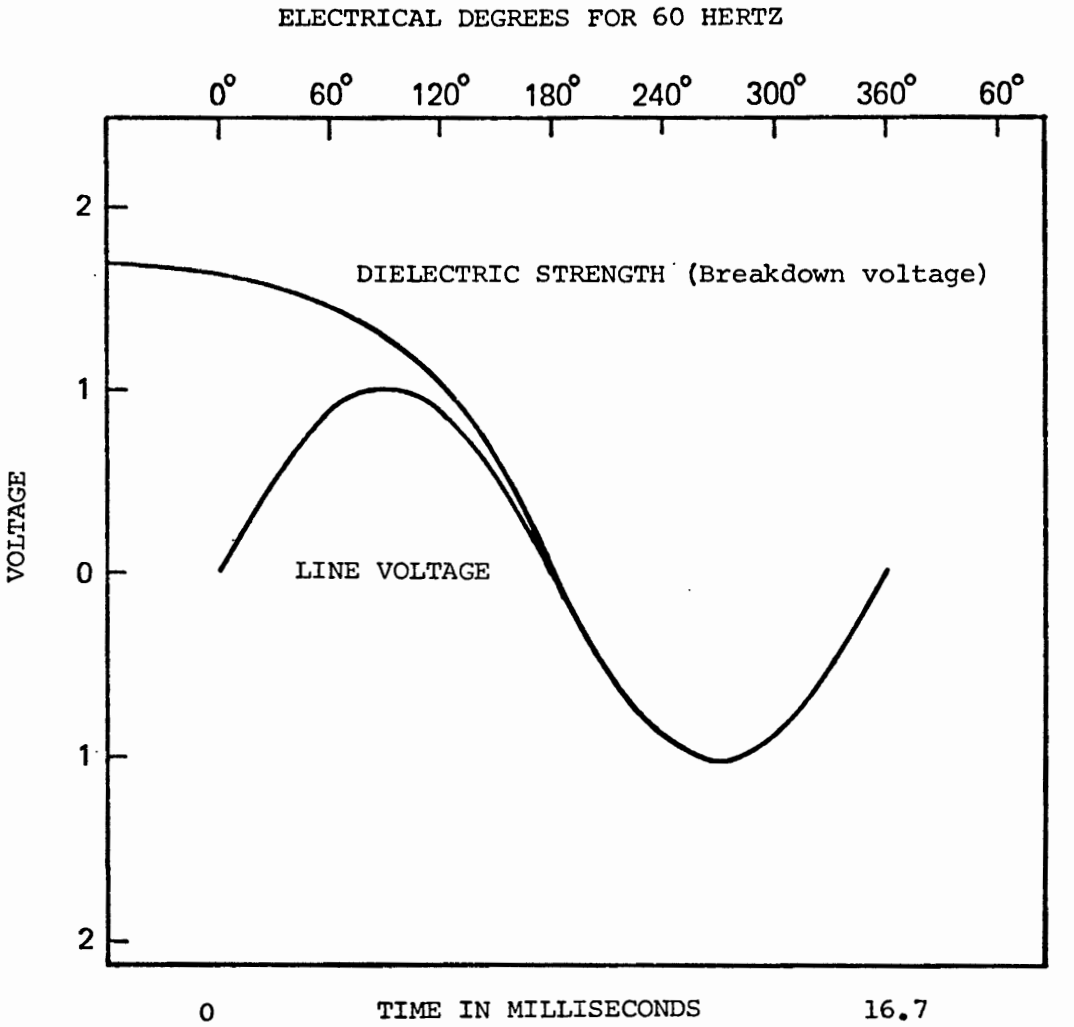

Figure 12 The sine wave represents the 60 Hz. voltage as a function of time. The other curve is of the necessary dielectric strength of the switching device, as a function of time, to allow energization at voltage zero.

30,500 kV/ft.(16) This means that a contact speed of 2.46 feet per second would allow synchronous switching on a 230 kV System. Fortunately, the contact speed of commercially available vacuum breakers exceeds this by a comfortable margin.

The switch selected for this application needs to have the required timing accuracy and to be cost competitive with existing methods of limiting inrush transients. No commercially available device was found for synchronous switching. The in-house development of a device especially designed for this application was out of the question due to the cost and the lack of necessary facilities. The modification of a commercially available device was chosen as the most cost-effective solution.

The vacuum breaker chosen for the project was a 230 kV Joslyn VBU-3, F9 unit. The switch consists of nine series vacuum bottles with a single operator for each pole. Each contact moves only a very small distance (0.187 inches) which gives a total open gap distance of less than 1.7 inches.

The switch is closed by a solenoid and opened by springs. The opening springs are charged during the close operation and for opening a trip solenoid pulls a latch, to activate the springs. The closing solenoid is powered from large capacitors which are charged from the station battery supply. The peak current of 55 amperes per phase which each solenoid draws makes this local energy storage necessary. The vacuum breaker is specified by the manufacturer to close in 4 to 6 cycles total time and trip in less than 1 cycle (at 60 Hz.).

The dielectric strength of vacuum is very high as is its rate of rise of dielectric strength. This makes the vacuum interrupter almost

restrike free, but also creates a new set of problems. The butt type contacts that have to be used in vacuum to avoid cold welding of metals are prone to bouncing(16,17). When contact bounce or prestrike occurs the high inrush current for capacitor bank energization is interrupted and high frequency transients are generated. These transients can cause extremely high overvoltages(17,18). This problem has been eliminated (according to manufacturers) by increased contact velocity and additional damping to avoid bouncing. Field tests were used to determine the effectiveness of this modification and evaluate the performance of modern vacuum breakers.

To determine the vacuum breaker characteristics a series of laboratory tests were required. The vacuum interrupter was assembled at the High Voltage Laboratory of the BPA Dittmer Center near Vancouver, Washington. Tests were made to determine the closing time accuracy(19). Speed is helpful in obtaining closing time accuracy, but the necessary factor is repeatability. The closing time must be consistent over a range of control voltages as well as other operating conditions.

Tests were made with both low voltage (150 VDC) and rated voltage (133 kV line to ground) applied across the interrupter. The station battery control voltage was varied from 118 to 135 VDC during the tests. Environmental conditions, particular temperature varied very little during the tests.

At a constant control voltage, closing times varied over a range of 6.2 ms. The variation of the control voltage from 118 to 132 VDC caused an additional 3.5 ms of timing deviation. With 150 VDC applied across

the contacts of the interrupter 6.5 ms of contact bouncing was noted. Records made at rated voltage did not provide enough data to discern the difference between contact bounce and prestrike. This performance would, of course, not meet the 1 ms value needed for synchronous switching.

A study was then made to determine the cause of the timing deviations. One cause was already known to be variations in the control voltage. The major source of timing deviation was traced to the closing contactor. This relay had more timing deviation than the interrupter and took longer to operate. The contactor contacts move farther than the vacuum interrupter contact.

The total close time of the unit was found to be slightly over 4.5 cycles (at 60 Hz.) which explained the 4 to 6 cycle closing time specified by the manufacturer. The interrupter alone closes in just over 1 cycle. The trip time is just under 1 cycle. Prestrike caused a 1 ms change in timing at rated peak voltage.

Two changes were made to improve the timing accuracy and repeatability. First the voltage on the energy storage capacitor for the closing solenoid was regulated. Second the circuit for energizing the solenoid was changed to a two step operation. The first step energizes the contactor which switches the capacitors from their charging circuit to their connection in series with the solenoid. The second step fires an electronic switch (SCR) to energize the solenoid at precisely the right time.

A voltage regulator was installed in the circuit that charges the energy storage capacitors. This regulator was designed specifically to charge capacitors and maintains a fixed voltage on the capacitors after

charging them. Although the close solenoids draw 55 amperes each, the capacitors charging current is limited to less than 1 ampere for all three poles, so the regulator is relatively inexpensive.

To reduce the timing errors introduced by the closing contactor a silicon controlled rectifier (SCR) was added in series with each contactor for each phase. A second closing signal was then supplied. The first closing signal activates the contactors, but the close solenoids are not energized as the SCR's blocked the current. The second close signal is then supplied, but delayed enough from the first to allow the slow operating contactors to close. This second signal turns on the SCR's, completing the circuit and closing the interrupter. The interrupter was then retested. See appendix II for details of the modifications.

The tests now demonstrated that even with control voltage variations, as before, the closing time changed less than $\pm$ 0.25 ms. This performance was good enough to equal that of the preinsertion resistors. Although it was not expected that this accuracy could be maintained in a field environment, the proposed accuracy of $\pm$ 1.0 ms could be expected to be attainable in practice.

Temperature-induced timing deviations had not been explored. One possible source of timing deviation identified was the thermal variations of the capacitance of the energy storage capacitors. Electrolytic capacitors change value significantly with temperature.

A mathematical model for the system was written (Appendix II) but numerical values for the parameters and components were not readily available. In discussions with the manufacturer it was discovered that, although they had performed environmental tests but these had not

included timing tests. Thermal expansion had been a problem, and the coefficients for the materials, which were developed for the manufacturer, were not available.

It was seen that mathematical analysis could not yield accurate enough results without more reliable component information. As no environmental test facility was available, the thermal effects would have to be evaluated during the prototype evaluation over a long enough time period to experience seasonal variations. If the device's performance was not within limits, a temperature sensitive circuit would need to be incorporated in the voltage regulator circuit to compensate for thermal variation.

With the modifications incorporated, a prototype was built and retested. The scheme was now ready for field tests, switching an actual system capacitor bank.

CHAPTER IV

FIELD TESTS

A prototype of the modified vacuum circuit breaker was built and given a field test to confirm the predicted performance when actually connecting capacitors to a high voltage circuit.

For comparison with the zero-voltage-closing vacuum breaker Fig. 16, results are shown using an unaltered connector, Fig. 14 and a preinsertion resistor, Fig. 15.

The location selected for the field tests was the capacitor Group 2, Section 4 at the J.D. Ross Substation near Vancouver, Washington(21). Capacitor Group 2 consists of two 59.4 MVAR sections and two 61.2 MVAR sections. The two sections that were involved in the tests were Sections 1 and 4, both 59.4 MVAR sections.

The modified vacuum breaker was temporarily installed in series with the existing device, a load break switch. Figure 13 shows the temporarily installed breaker. The load break switch was equipped with 66 ohm preinsertion resistors. An arcing horn was removed during the test to allow performance without preinsertion resistors to be determined. The load break with arcing horn removed is shown in Figure 11.

The capacitor bank was instrumented as indicated in detail in Appendix III. It consisted basically of bus voltage and current measurements as well as measurements of step and touch potentials(22).

The vacuum breaker operation, as well as many other test functions such as oscillograph start and stop, was controlled by a power sequence

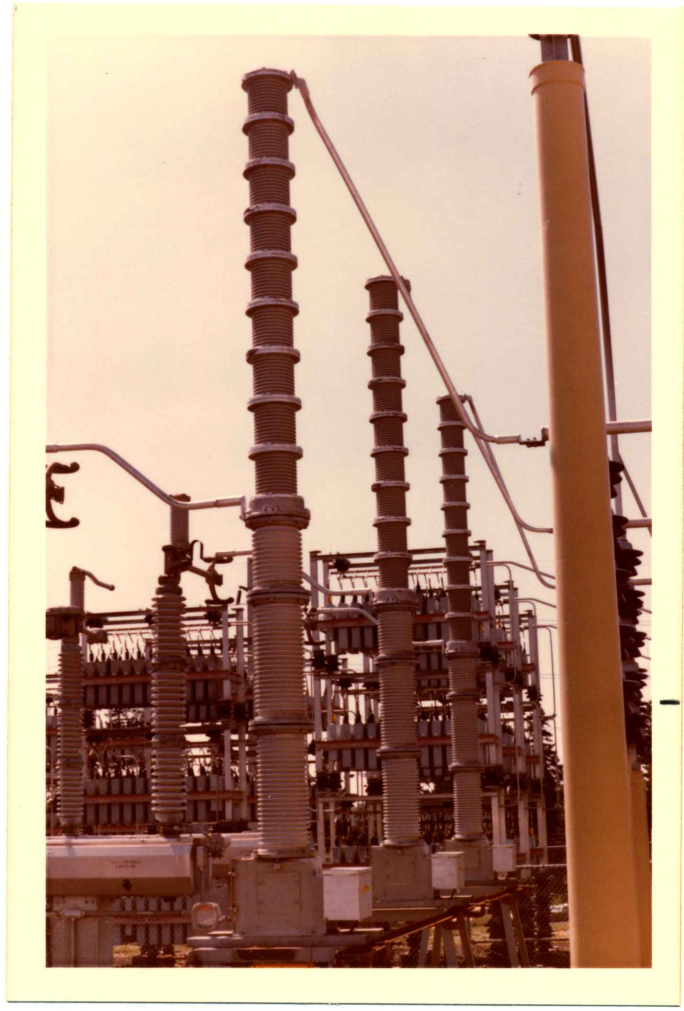

Figure 13 The vacuum breaker temporarily installed at Ross Substation for the field tests.

controller. This device offers programmable relays that open and close within 160 ms of the preset time. A synchronizing signal for the programmer was obtained from the A phase bus voltage.

To reduce possible transient potential problems, the vacuum breaker was operated from a portable station battery and the test equipment power was supplied by an engine-generator. Appendix III contains details of the test setup.

Single Bank Case

The tests were completed and the data analyzed. A listing of data can be found in Appendix IV. The test results closely followed the results of the studies.

During the single bank portion of the test the primary transient frequency was 1.0 kHz (Figure 22).

When the vacuum breaker was energized near crest voltage, a prestrike and/or contact bounce phenomena resulted in a current interruption and second energization; this will be discussed later (Figure 22).

Back to Back Case

The back-to-back test series was also conducted. A complete listing of the data can be found in Appendix IV.

The frequency of the voltage transient was still 1 kHz.

The frequency of the current transient between the two capacitor banks was 12 kHz.

The peak inrush current data has been plotted as a function of the switch timing deviation from voltage zero for both the "single bank" (Figure 20) and the "back to back" (Figure 21) case. The data was

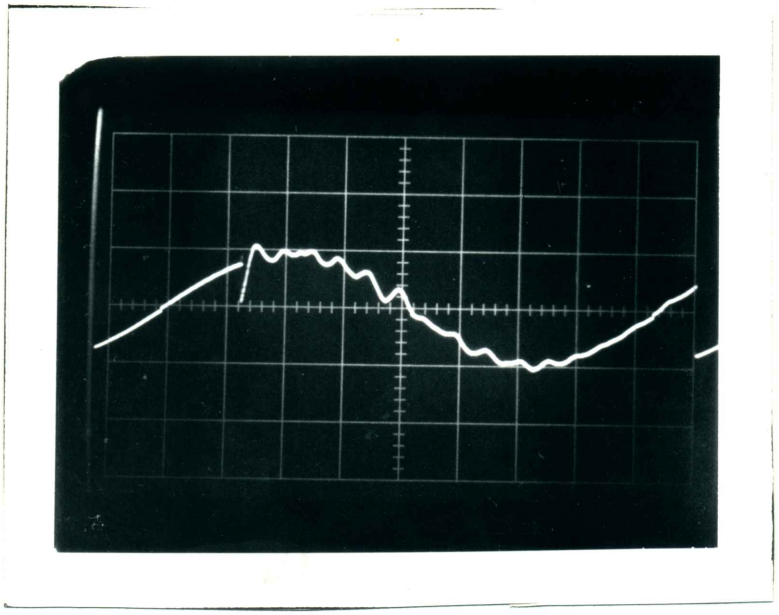

Figure 14 A phase bus voltage, single bank, load break switch without resistors. 204 kV/division, 2 ms/division.

Load Break Switch, no resistors (See Figure 14)

Energization occurred at or near a voltage peak causing a bus voltage dip of 1.0 per unit (p.u.) and a bus voltage overshoot to 1.4 p.u.

Peak current was 2700 amperes.

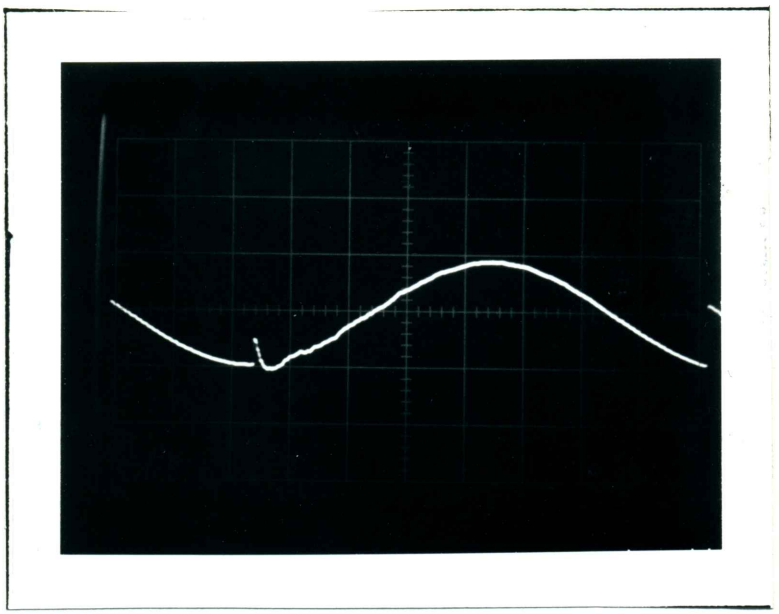

Figure 15 A phase bus voltage, single bank, load break switch with 66 ohm preinsertion resistors. 204 kV/division, 2 ms/division.

Load Break Switch with resistors (See Figure 15)

Energization occurred at or near peak voltage. The bus voltage dip was 0.6 p.u. and the overvoltage was 1.2 p.u. The peak current was 392 amperes.

During this test the preinsertion resistor on C phase was found to be misadjusted and did not insert. A portion of the test was redone after the problem was corrected.

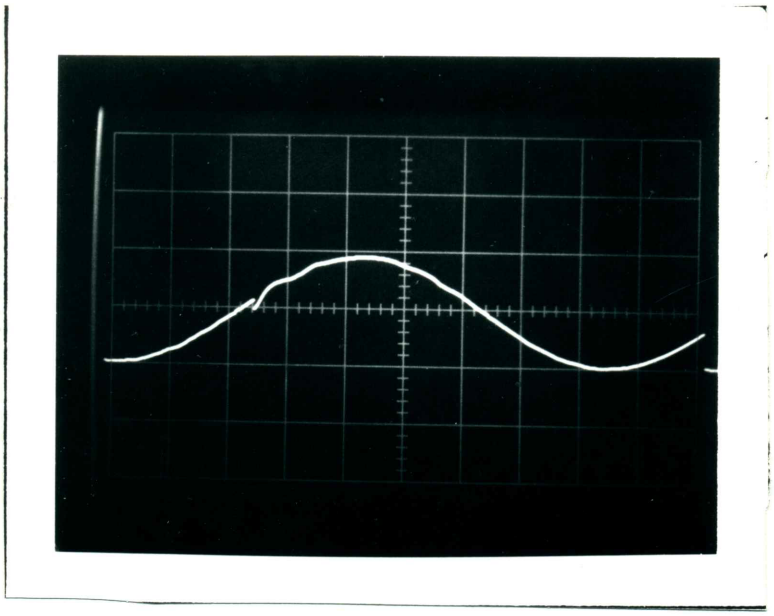

Figure 16 A phase bus voltage, single bank, vacuum breaker closed near voltage zero. 204 kV division, 2 ms division.

Vacuum Breaker at Voltage Zero (See Figure 16)

Attempts to energize the capacitor bank at the exact instant of voltage zero were not successful. Energization 0.2 ms from voltage zero was achieved. When energized near voltage zero (0.2 ms) the bus voltage dip was 0.05 p.u. There was no overvoltage unless deviations from voltage zero were set for over 1.3 ms.

Energization near voltage zero resulted in no voltage transient, only a phase shift is apparent.

The peak current was 390 amperes.

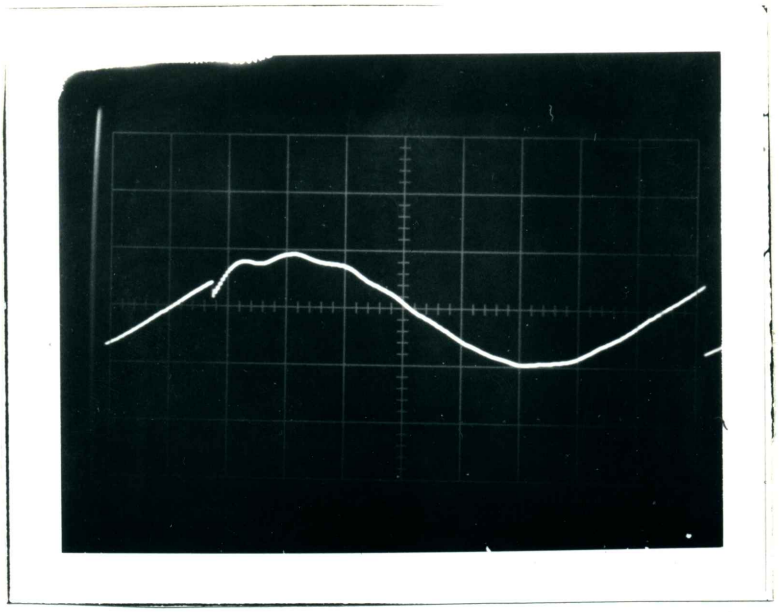

Figure 17 A phase bus voltage, back to back, load break without resistors. 204 kV/division, 2 ms/division.

Load Break Switch, no resistors (see Figure 17)

The bus voltage dip was 0.6 p.u. and the peak overshoot was 1.3 p.u. Energization was near peak voltage. The peak inrush current was 24,500 amperes.

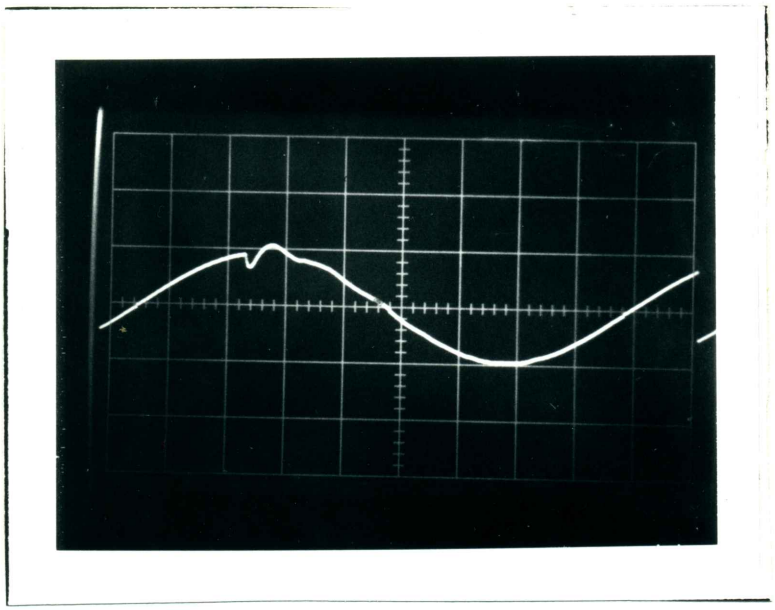

Figure 18 A phase bus voltage, back to back, load break switch with 66 ohm preinsertion resistor. 204 kV division, 2 ms division.

Load Break Switch with resistors (See Figure 18)

Energization was near crest voltage and the voltage dip was 0.3 p.u. The bus overvoltage was 1.1 p.u. The peak inrush current was 2,750 amperes.

The peak current on resistor bypass was measured at 2,000 amperes.

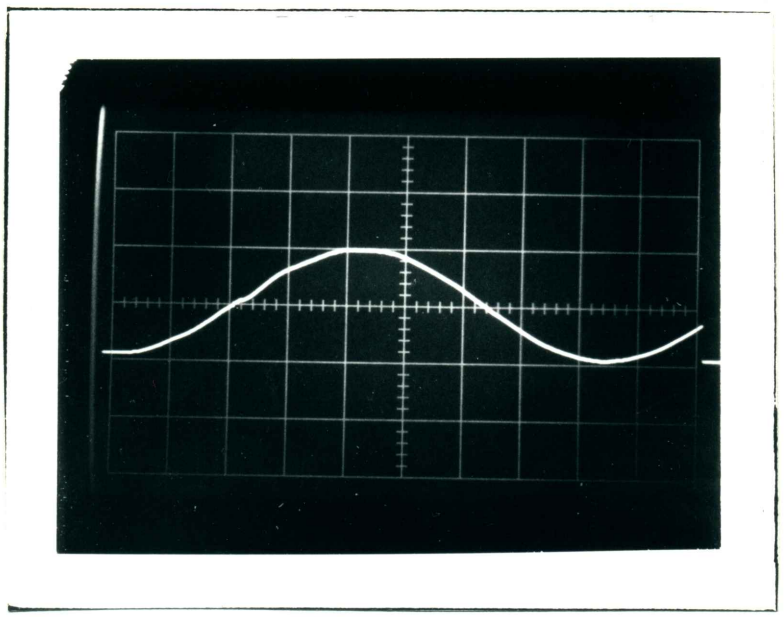

Figure 19 A phase bus voltage, back to back, vacuum breaker at voltage zero. 204 kV division, 2 ms division.

Vacuum Breaker near voltage zero (See Figure 19)

Closure very near voltage zero was achieved.

The bus voltage dip was unmeasurable.

There was no overvoltage unless the breaker was set to close more than 1.7 ms from voltage zero.

The peak inrush current was from 1,630 to 2,450 amperes when the capacitor bank was energized at or near voltage zero.

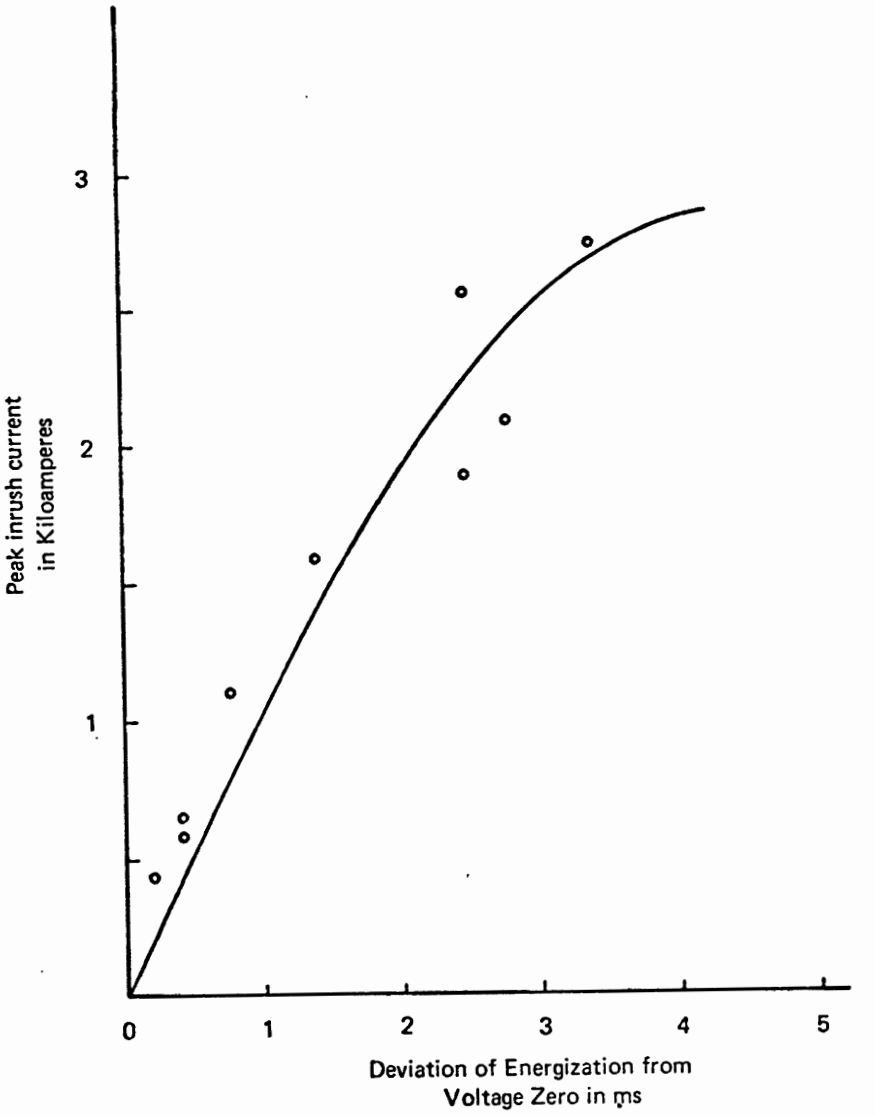

Figure 20 The measured values of peak inrush current (points) plotted with the calculated values (line) from Figure 9, for the "single bank" case.

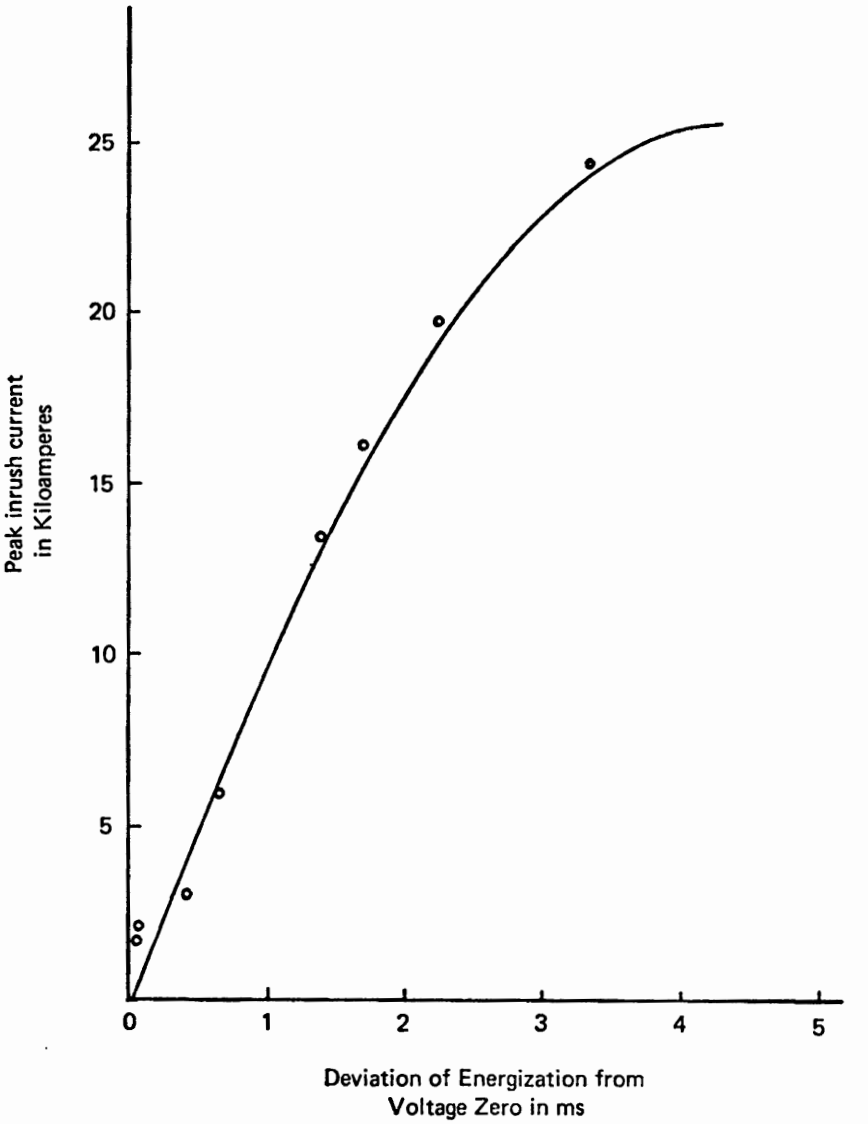

Figure 21 The measured values of peak inrush current (points) plotted with the calculated values (line) from Figure 10, for the "back to back" case.

plotted over curves of the calculated values that were plotted in Chapter 2 (Figures 9 and 10). The test data confirms the calculated values.

The results of the step and touch potential measurements are given in detail in Appendix IV. Closure at voltage zero was far more effective in reducing Electro-Magnetic Interference (EMI) levels than preinsertion resistors. For example, during the back to back portion of the test the touch potential was 912 volts without resistors, 180 volts with resistors and 6 volts when energized at voltage zero. It is interesting to note that on this and other EMI measurements the EMI levels are not strictly related to peak inrush current as might be expected. The reason for this is not clear, but the vacuum breaker produced lower EMI levels than the load break when the inrush currents had the same peak values. One possibility is an effect caused by the nonlinearities of the air arc and higher frequency components.

Some difficulty was experienced while attempting to make minor timing adjustments near voltage zero. A minor change would seem to have little if any effect. Adjustment seemed to be more difficult during the single bank switching than during back to back. The problems may be caused by contact bouncing. When a low voltage (as near voltage zero) is across the contacts, a very small current flow is established but is immediately interrupted, and measureable current is not established until the voltage is of sufficient magnitude to establish arcing. During the back to back switching the higher currents help maintain the arc and reduce the effect.

During tests when the vacuum breaker was closed near crest voltage another phencmena was observed. This occurred on both single bank and

back to back tests. Prestrike and/or contact bounce resulted in an interruption shortly after energization. When a high frequency current zero occurred, the vacuum breaker interrupted the current because metallic contact was not yet completed. A second energization occurred approximately 1 ms later. This did not result in any high overvoltages in this case. Figure 22 is a voltage and current waveform oscillographic test record which illustrates the phenomena.

The field tests had demonstrated the technical feasibility of controlled closing as a method to reduce inrush transients. There were still some unanswered questions about the practicality of this method. The effects of temperature on closing time were still not known. The effect of electromagnetic interference on the electronics in the closing circuitry of the vacuum breaker had not yet been determined. The maintenance requirements of the vacuum breaker when closing timing accuracy must be maintained were not predictable. These questions could only be answered by a long-term, inservice evaluation.

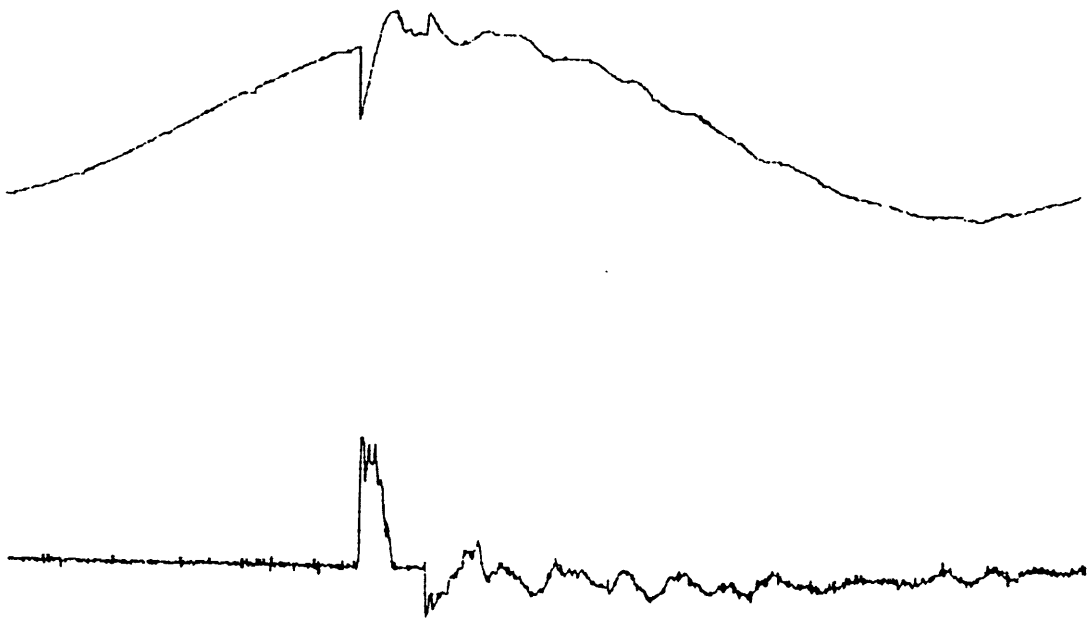

Figure 22 Bus voltage (above) and current (below) during a "single bank" energization. Note the interruption of current caused by prestrike or contact bouncing.

CHAPTER V

THE PROTOTYPE INSTALLATION

To determine the effects of time and environment on the performance the prototype is undergoing a long-term evaluation.

The BPA D.R. Keeler Substation was choosen for the long-term evaluation.

Figure 23 shows the installation. This picture and an early draft of this thesis were furnished to Electrical World Magazine for the information on which an article in their January 1979 issue was based(23).

The manufacturer of the vacuum breaker had redesigned his product and the new model is much less prone to the contact bounce that had been noted during the testing. The early model vacuum breaker was returned to the factory to have the new design changes incorporated into it.

A BPA Controlled Closing Device was modified for this application. An interface/driver circuit was designed and built to couple the control device to the SCR's (Appendix II).

Other minor changes were necessary in the control circuitry to prevent misoperation and allow normal relaying functions. See Appendix II for details of the modifications.

The vacuum breaker was operated almost every day for 2 years. When temperatures were at extremes, an oscillographic record of the bus voltage was made during a single bank switching operation and the timing variations of the breaker determined. A sample oscillogram is provided in Figure 24. The timing of the vacuum deviated plus and minus 1 millisecond from 97°F to 28°F. The colder the temperature,

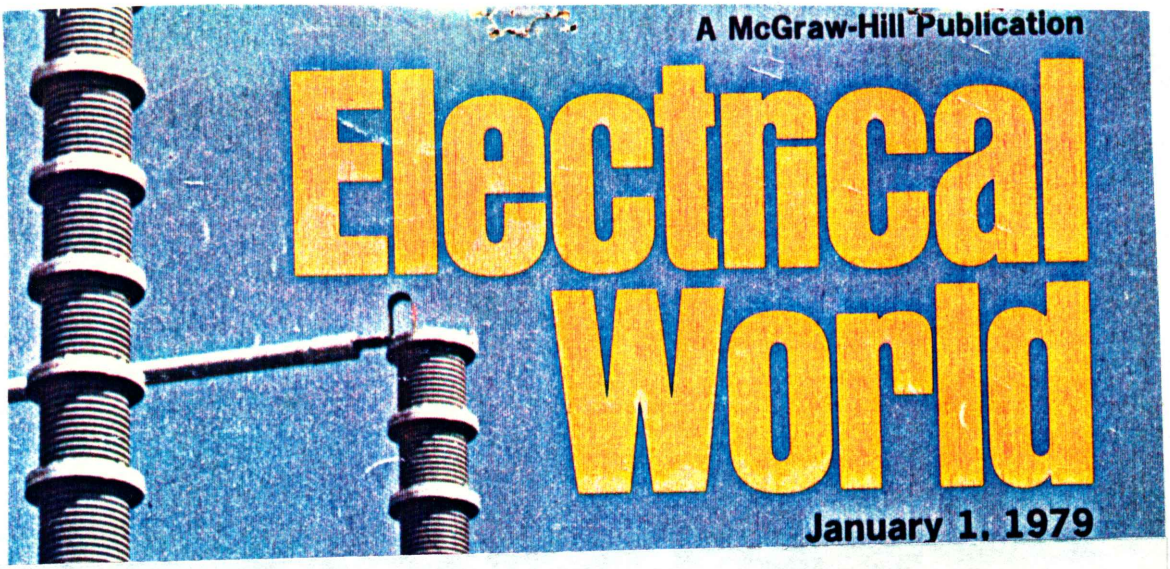

Figure 23 The permanently installed syncronously switching vacuum breaker. This photo was provided to Electrical World Magazine and appeared on the cover of the January 1, 1979 issue.

the faster the breaker operated. This indicates that the mechanical rather than the electrical circuit effects of temperature dominated.

We can note in Figure 24 that the 28°F reading it is not in agreement with the other points. The temperature of the breaker most probably was lagging behind the ambient temperature as the temperature a few hours before was 10°F.

The entire system has required no maintenance during the first 2 years. No timing deviation has been observed except that due to temperature changes. Figure 25 is a plot of the timing deviation as a function of temperature recorded during the first year of operation. Timing deviations were always within $\pm$1.0 ms.

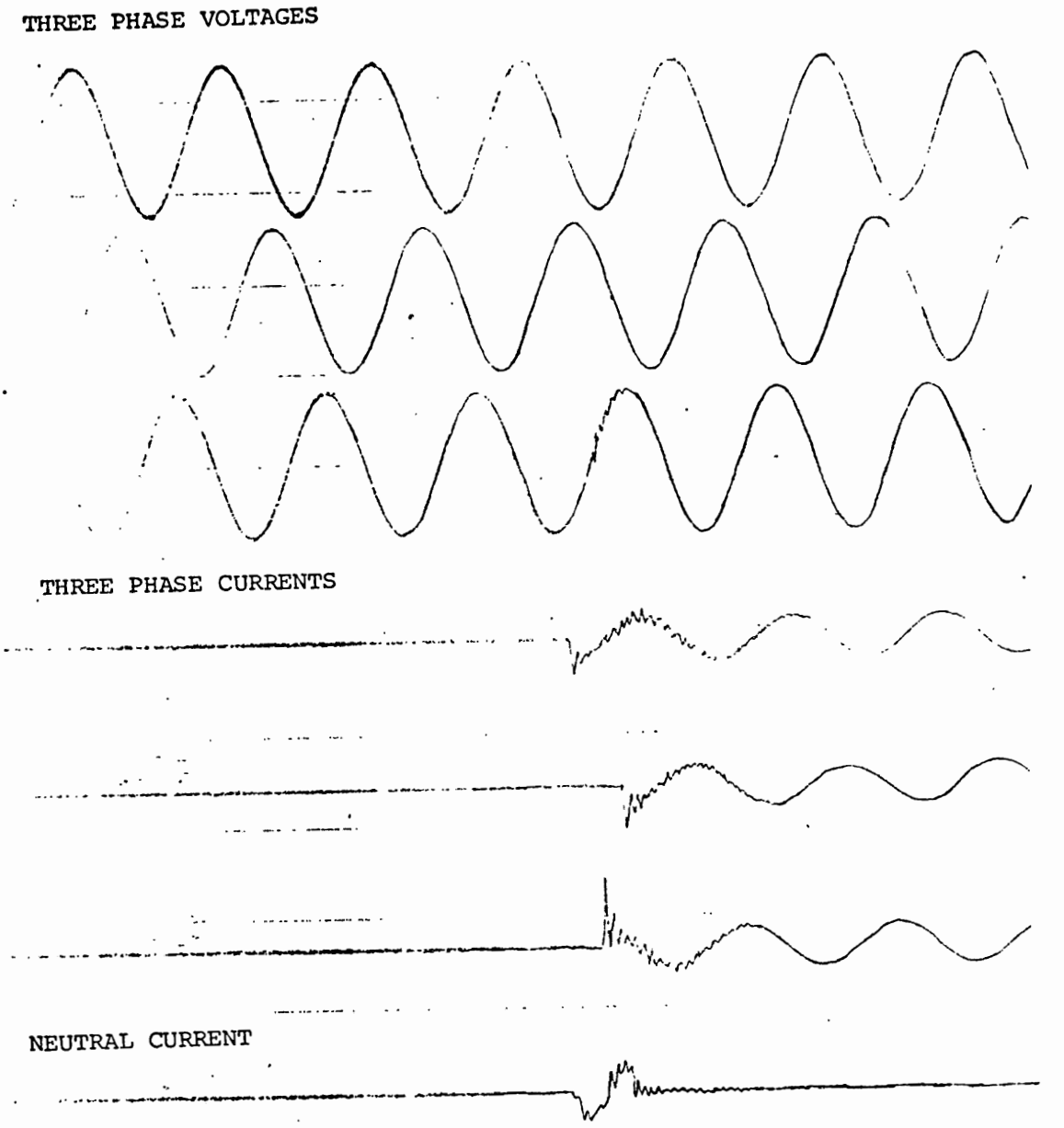

Figure 24 An oscillographic record of bus voltages and phase currents during a single bank energization of the prototype installation.

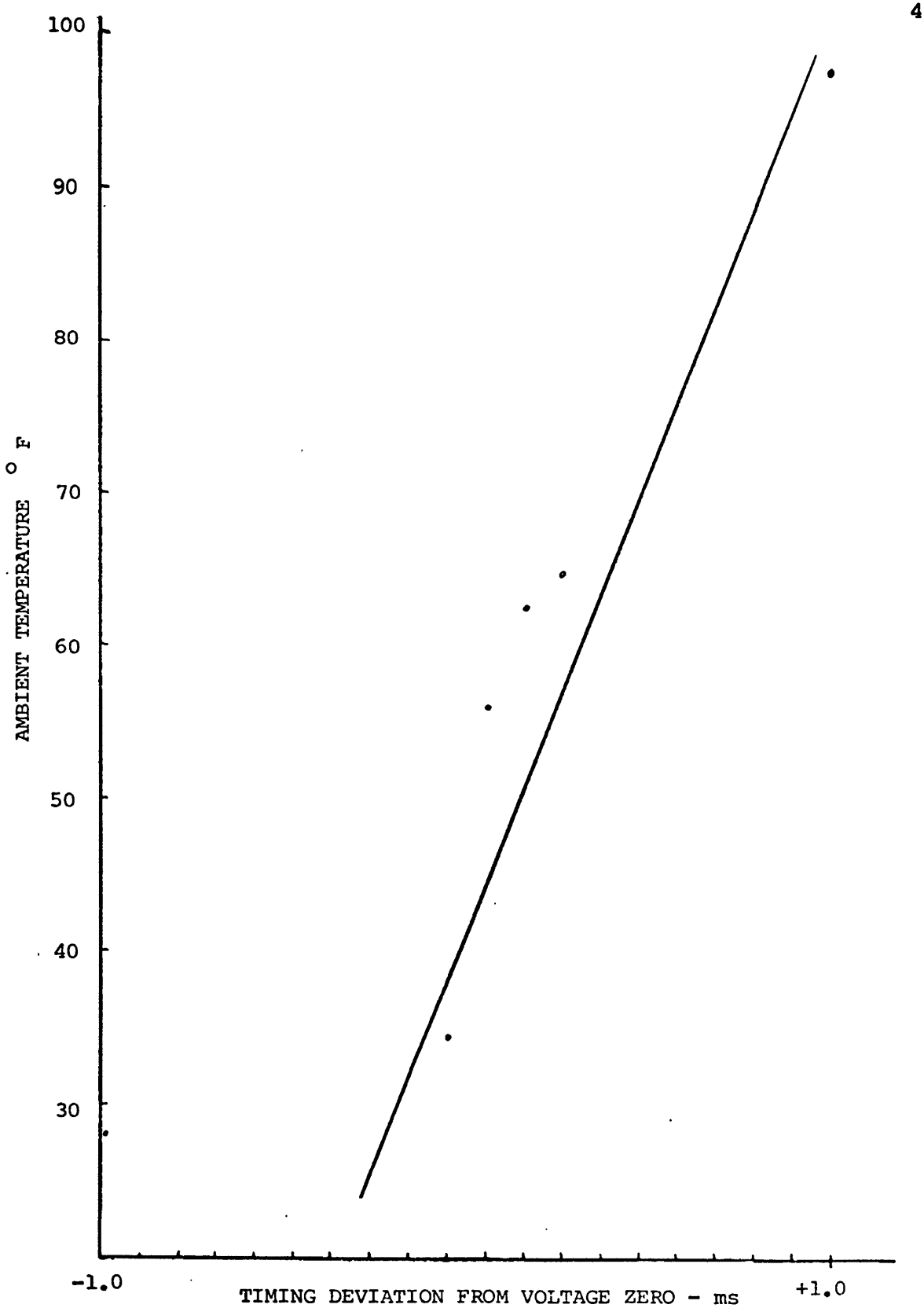

Figure 25 A plot illustrating the effects of ambient temperature on the timing accuracy of the switch during its first 2 years in service.

CHAPTER VI

CONCLUSIONS

The goal of this investigation, the development of a practical device for connecting power factor correcting capacitors to a very high voltage power system has been achieved. The cause of previous problems has been traced to severe switching transients. It has been shown that these transients can be minimized by making the capacitor connection at a time when the alternating voltage is near zero. A practical device has been designed, tested and is in regular operation, which accomplishes this zero-voltage-switching.

Field tests have verified the mathematical analysis. The transients generated during energization of power factor correction capacitors on a high voltage power transmission system can be reduced by energization at or near voltage zero. Present technology allows this technique to be not only feasible, but practical and economical.

The energization of shunt capacitors near voltage zero results in reduced transient levels. Reductions in magnitudes of voltage transients as well as current transients are accomplished. Dangerous step and touch potential magnitudes are also reduced to safe levels. The frequency characteristics of the transients produced are not appreciably changed, but the magnitudes are greatly reduced. The magnitude of the transient has been shown to be proportional to the magnitude of the bus voltage at the instant of energization, as might be expected. By switching within ± 1.0 ms of voltage-zero the maximum transient magnitude can be reduced to less than 37 percent of that caused by closing at maximum voltage. Overvoltages are eliminated

because the voltage transients are not only reduced, but they occur at a time when the line voltage to which they add is lower.

The magnitude of the transients has been shown to be proportional to the magnitude of the bus voltage at the instant of energization as might be expected. This gives a minimum 63 percent reduction in transient magnitudes from the worst case if energization occurs within $\pm$1.0 ms of voltage zero. This timing accuracy also eliminates overvoltages.

A conventional vacuum breaker with minor modifications to its control circuitry and the addition of a control device can perform adequately to switch shunt capacitors synchronously. The scheme is economically competitive with other transient reduction schemes, considering initial cost and maintenance (annual) costs. A switching device with its mechanical system designed specially for synchronous switching could improve performance even further, but does not appear worth the investment considering the performance level obtained by modifying the available device.

The vacuum breaker has advantages over other switching devices. The vacuum breaker operates with a lower sound level and does not have the bright flash of an air arc. This could make it desirable for use at a substation near a residential area. The elimination of the air arc also eliminates the possibility of the hot gasses being blown and causing a phase to phase fault as has happened on the BPA system.

As synchronous switching is possible, other applications come to mind. One might detect the polarity of the residual magnetism of a transformer and energize it with the proper polarity to reduce the

magnetization inrush currents. Another application might be in reclosing on a high speed generator to reduce shaft stresses and mechanical oscillations.

REFERENCES

(1) Konkel, H. E., Legate, A. C., and Ramberg, H. C., "Limiting Switching Surge Overvoltages with Conventional Power Circuit Breakers," IEEE Transactions on Power Apparatus and Systems, Vol. PAS-96, pp. 535, Mar./Apr. 1977.

(2) Frank, H. and Landstrom, B., "Power Factor Correction with Thyristor Controlled Capacitors," ASEA Journal, Vol. 44, No. 6, pp. 180-184, 1971.

(3) Brunke, J. H. and Schockelt, G. G., "Synchronous Energization at Shunt Capacitors at 230 kV," IEEE Paper No. A78 148 9, 1978.

(4) Svensen, O. H., "The Influence of Prestrike on the Peak Values of Energization Transients," IEEE Transactions on Power Apparatus and Systems, Vol. PAS-95, pp. 711 720, Mar./Apr. 1976.

(5) Boehne, E. W., "EHV Surge Suppression on Interrupting Light Currents with Air Switches, I-Capacitive Currents," IEEE Transactions on Power Apparatus and Systems, Vol. PAS-84, No. 10, pp. 906-923, October 1965.

(6) Boehne, E. W., "Energization Surges in Capacitive Circuits," IEEE Paper No. 70 CP 235 PWR, 1970.

(7) Boehne, E. W., "Surge Phenomena Associated with the Energization of Capacitive Circuits," presented at the Power System Overvoltages Symposium, University of Manchester, Sept. 1974.

(8) Pflanz, H. M. and Lester, G. N., "Control of Overvoltages on Energizing Capacitor Banks," IEEE Transactions on Power Apparatus and Systems, Vol. PAS-92, pp. 907-915, May/June 1973.

(9) Pflanz, H. M., "Generation of High Voltages on Energizing Capacitive Circuits," presented to the International Symposium on High Voltage Technology, Munich, 1972.

(10) ANSI C37.0731-1973 "Application Guide for Capacitance Current Switching For AC High Voltage Circuit Breakers Rated on a Symmetrical Current Basis," pp. 14-20.

(11) Dommel, H. W., "Digital Computer Solution of Electromagnetic Transients in Single and Multiphase Networks," IEEE Transactions on Power Apparatus and Systems, Vol. PAS-88, pp. 388-399, April 1969.

(12) Wiitanen, D. O. and Morgan, J. D., "Models for Predicting Capacitor Bank Switching Transients," IEEE Paper No. 70 C 5 P493 497, 1970.

(13) Rogers, E. J., and Gillies, D. A., "Shunt Capacitor Switching EMI Voltages, Their Reduction in Bonneville Power Administration

Substation," IEEE Transaction on Power Apparatus and Systems, Vol. PAS-93, pp. 1849-1860, Nov./Dec. 1974.

(14) Gillies, D. A., Rogers, E. J., and Ramberg H. C., "Transient Voltages, High Voltage Capacitor Switching," Presented to the 12th Annual Conference for Protective Relay Engineers, Texas A&M, 1967.

(15) Solorzano, E. F., and Rush, P. L., "Application of Load Break Swtiches For Switching High-Voltage AC Shunt Capacitor Banks," IEEE Transactions on Power Apparatus and Systems, Vol. PAS-89, pp. 1504-1510, July/Aug. 1970.

(16) Selzer, A., "Switching in Vacuum, A Review," IEEE Spectrum, pp. 26-37, June 1971.

(17) Barkan, P., "A Study of Contact Bounce Phenomenon," IEEE Transactions on Power Apparatus and Systems, Vol. PAS-86, No. 2, pp 231-240, February 1967.

(18) Boehne, E. W. and Low, S. S., "Shunt Capacitor Energization with Vacuum Interrupters-A Possible Source of Overvoltage," IEEE Transactions on Power Apparatus and Systems, Vol. PAS-88, No. 9, pp. 1424-1443, September 1969.

(19) Pflanz, H. M., "Analysis of Multiple Prestrike and Interruption Phenomena in Capacitive Circuits," IEEE Transactions on Power Apparatus and Systems, Vol. PAS-91, pp. 2262, Nov./Dec. 1972.

(20) Connelly, J. W., "Laboratory Report 38579 EO Requested by J. H. Brunke," Dec. 1975.

(21) Brunke, J. H., "Voltage Zero Shunt Capacitor Switching Test, Ross Substation," BPA Test Report, June 1976.

(22) Rogers, E. J., "EMI and Transient Control by Point on Wave Energization of Shunt Capacitors," Memo to F. G. Schaufelberger, June 8, 1976.

(23) Wolff, R. F., "Control of Capacitor Closing Nips Surges," Electrical World, Jan. 1, 1979, pp. 38-40.

(24) Del Toro, V., "Electromechanical Devices for Energy Conversion and Control Systems," Prentice-Hall, (Englewood Cliffs, N. J., 1968), pp. 44-49).

(25) Fitzgerald & Kingsley., "Electric Machinery," Third Edition, McGraw-Hill, (New York, N.Y., 1971), pp. 107-113.

(26) Roger, E. J., "Multi-element Coaxial Shunt," IEEE Transactions on Power Apparatus and Systems, Vol. PAS-93, pp. 1743, Nov./Dec. 1974.

(27) Fillenberg, R. R. et. al., "Exploration of Transients By Switching Capacitors," IEEE Transaction on Power Apparatus and Systems, Vol. PAS-90, pp. 250-260, Jan./Feb. 1971.

(28) Rogers, E. J., "Instrumentation Techniques in High Voltage Substations, Part I, and Part II," IEEE Transactions on Power Apparatus and Systems, Vol. PAS-92, pp. 127-131, pp. 132-138, Jan/Feb. 1973.

(29) Singer, R. E., "Some Unique Properties of Vacuum Interrupters," Circuit Breakers 38A1C71, Section 5, pp. 901-905, 1971.

(30) Colclaser, R. G., Wagner, L. L., Donohue, E. D., "Multi-Step Resistor Control at Switching Surges," IEEE Transactions of Power Apparatus and Systems, Vol. PAS-88, pp. 1022-1028, July 1969.

(31) Beehler, J. and McConnell, L. D., "A New Synchronous Circuit Breaker For Machine Protection," IEEE Transactions on Power Apparatus and Systems, Vol. PAS-92, pp. 668-672, Mar/Apr. 1973.

(32) Greenwood, A. H. et. al., "A Guide to the Application of Vacuum Circuit Breakers," IEEE Transactions on Power Apparatus and Systems, Vol. PAS-90, pp. 1589-1597, July/Aug. 1971.

APPENDIX I

COMPUTER STUDIES

The anticipated switching transients were determined by the computer analysis of a circuit model based on expected component performance and values.

The studies were run on the BPA Cyber 70 (CDC6600) computer. The program is named the Electromagnetic Transients Program. The original program was developed by H. Dommell(11). It uses a trapozoidal method to obtain the solution. Output was in the form of voltage and current plots. Figures 26 through 45 show both back to back and single bank energizations at various phase angles.

Approximated parameters for a 230 kV bus and capacitor section were programmed. The time step was 25 ns. Both voltage and current waveforms were plotted. The calculations were done in per unit. Calculations were performed for both single bank and back to back cases.

One case was run for a delta connected capacitor bank, as is commonly used at lower voltages. In this case the first phase to close did not complete any circuit. The next two phases were closed, not at voltage zero, but when the voltage across the capacitive element was zero.

See Figure 44 for the voltage plot of the transient.

Figure 45 is a time expansion of the voltage transient when energizing a capacitor bank at voltage zero (back to back).

Figure 46 is the model used for the computer analysis including damping.

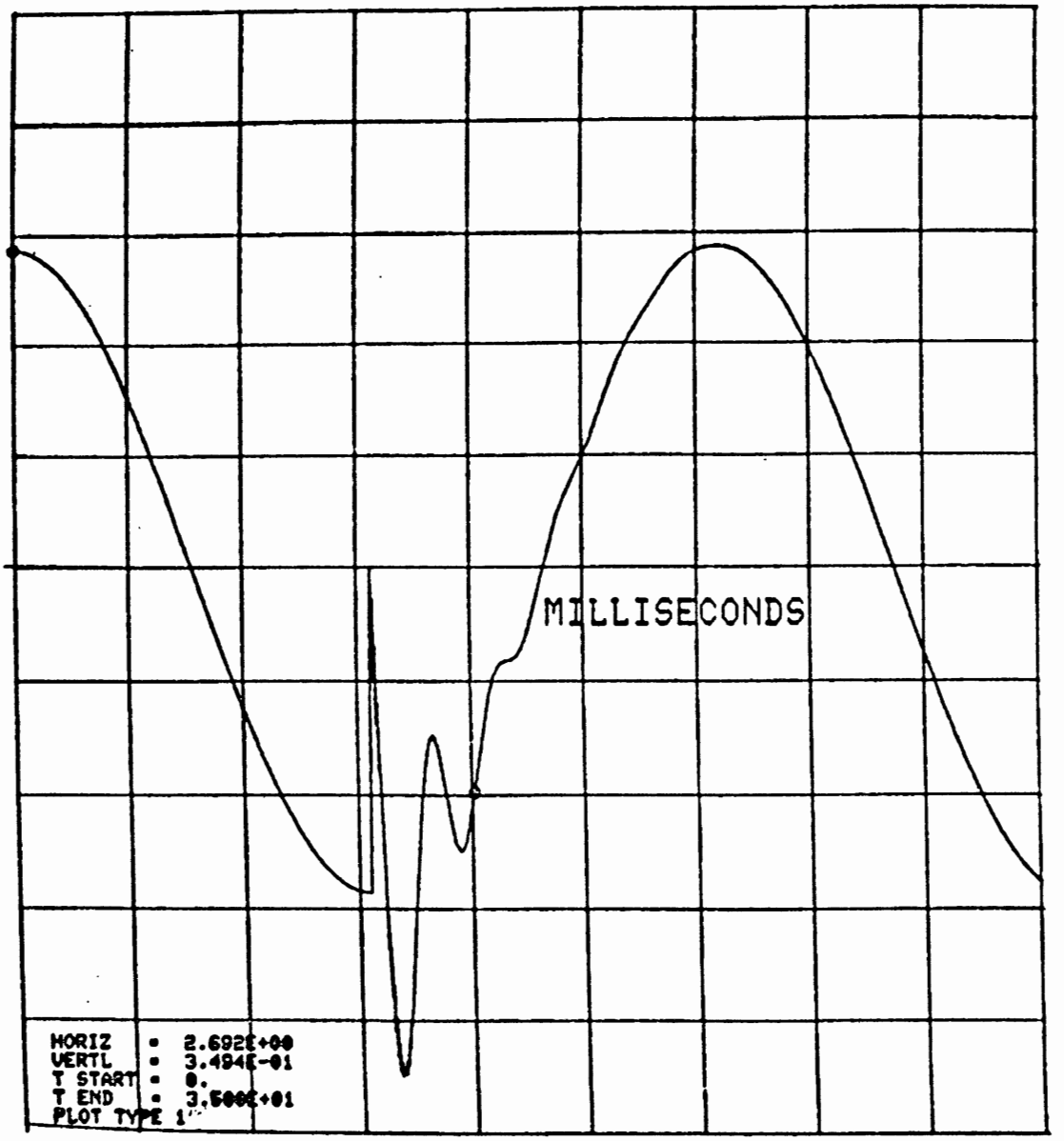

Figure 26 Computer plot of the bus voltage as a function of time for the "single bank" case. Energization 4.17 ms from voltage zero.

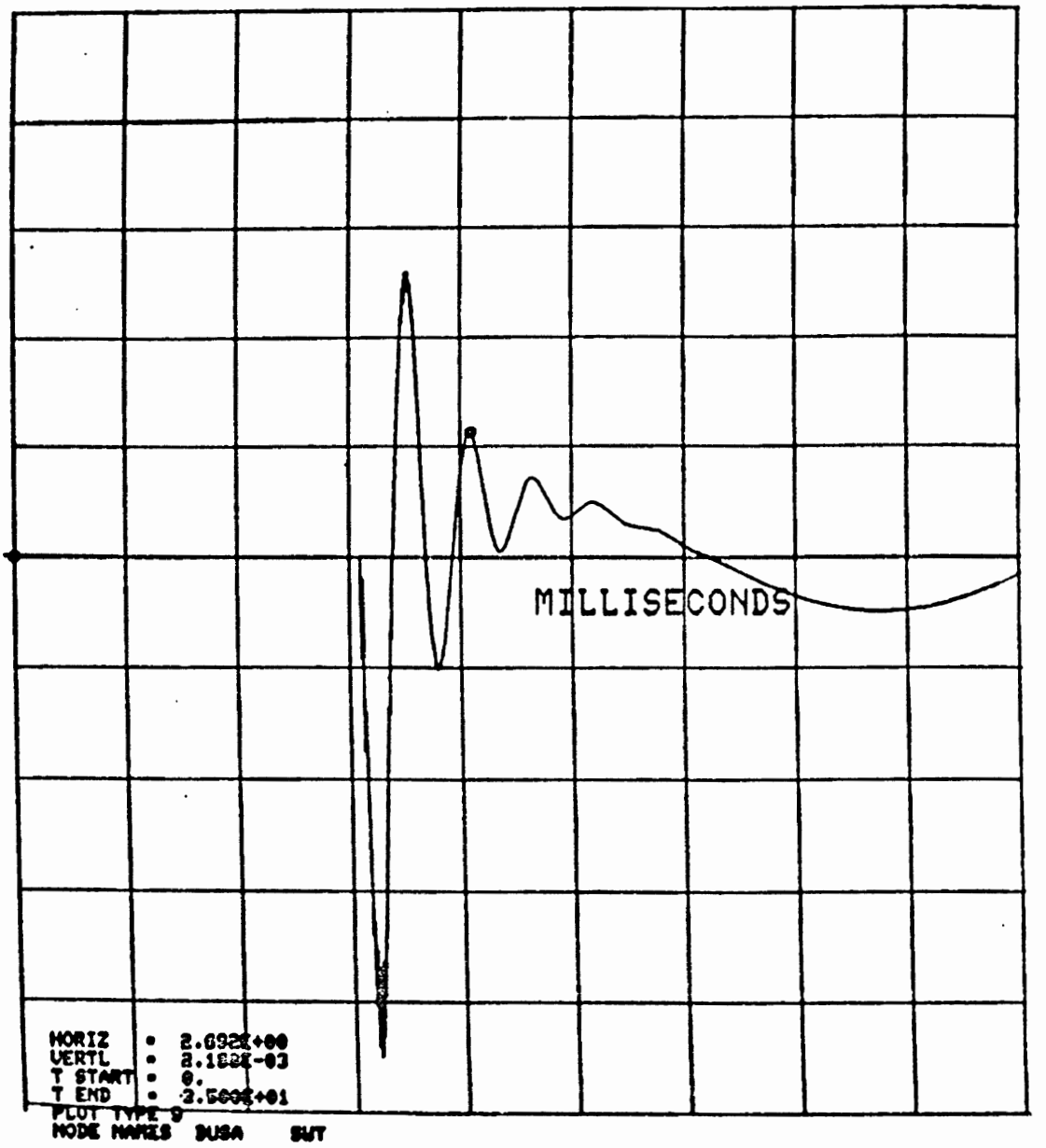

Figure 27 Computer plot of the capacitor current as a function of time for the "single bank" case. Energization 4.17 ms from voltage zero.

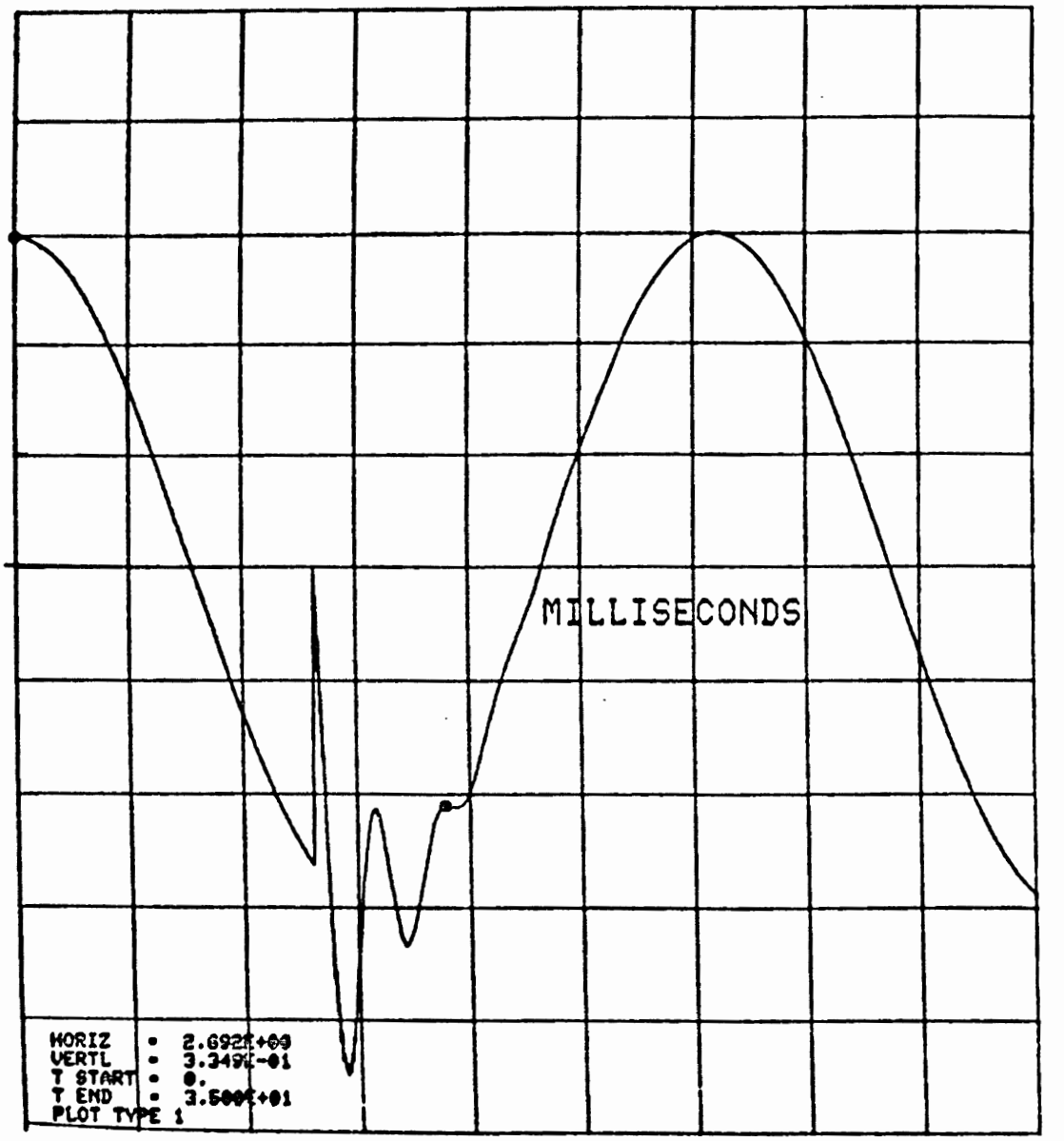

Figure 28 Computer plot of the bus voltage as a function of time for the "single bank" case. Energization 3.0 ms from voltage zero.

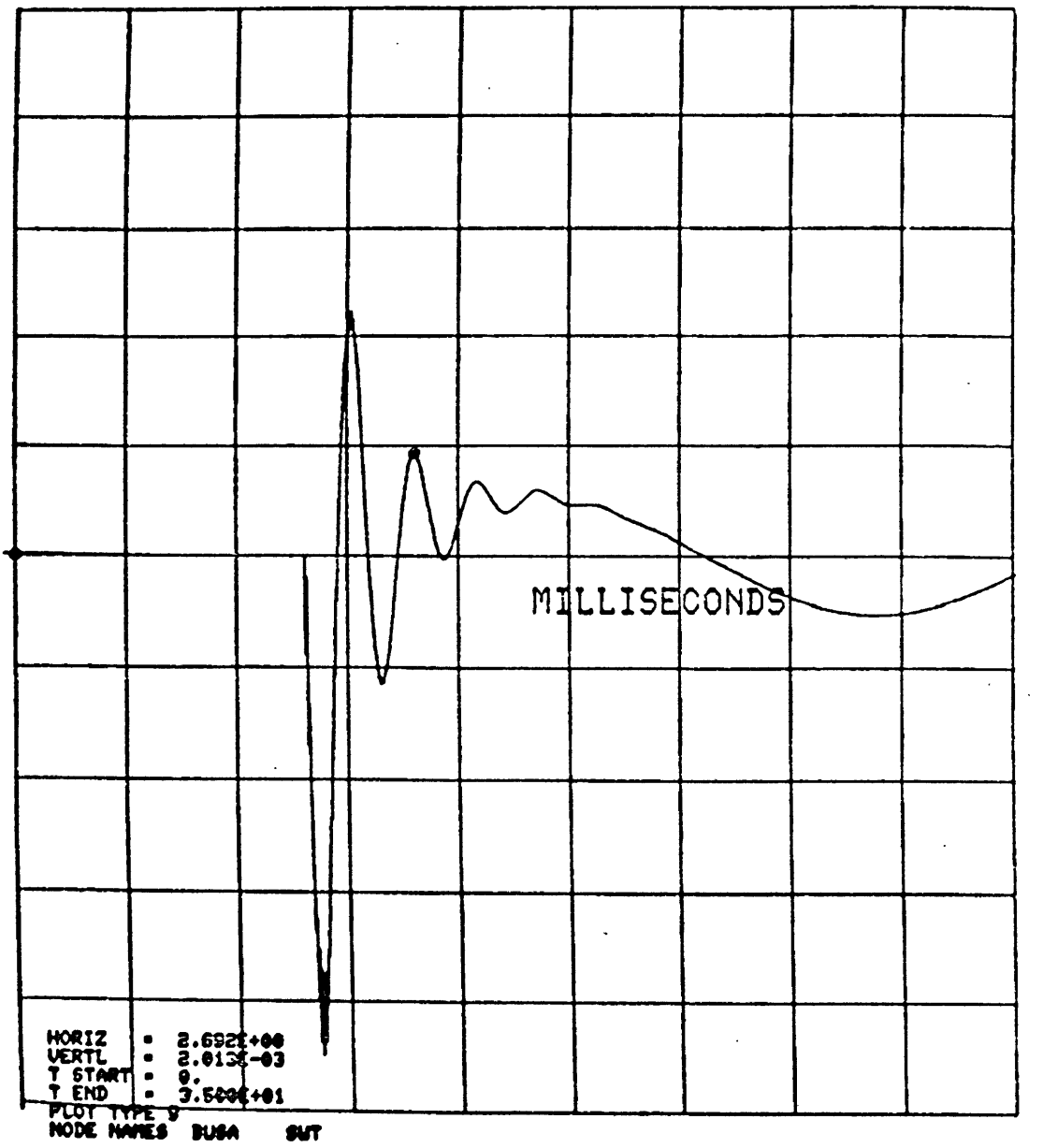

Figure 29 Computer plot of the capacitor current as a function of time for the "single bank" case. Energization 3.0 ms from voltage zero.

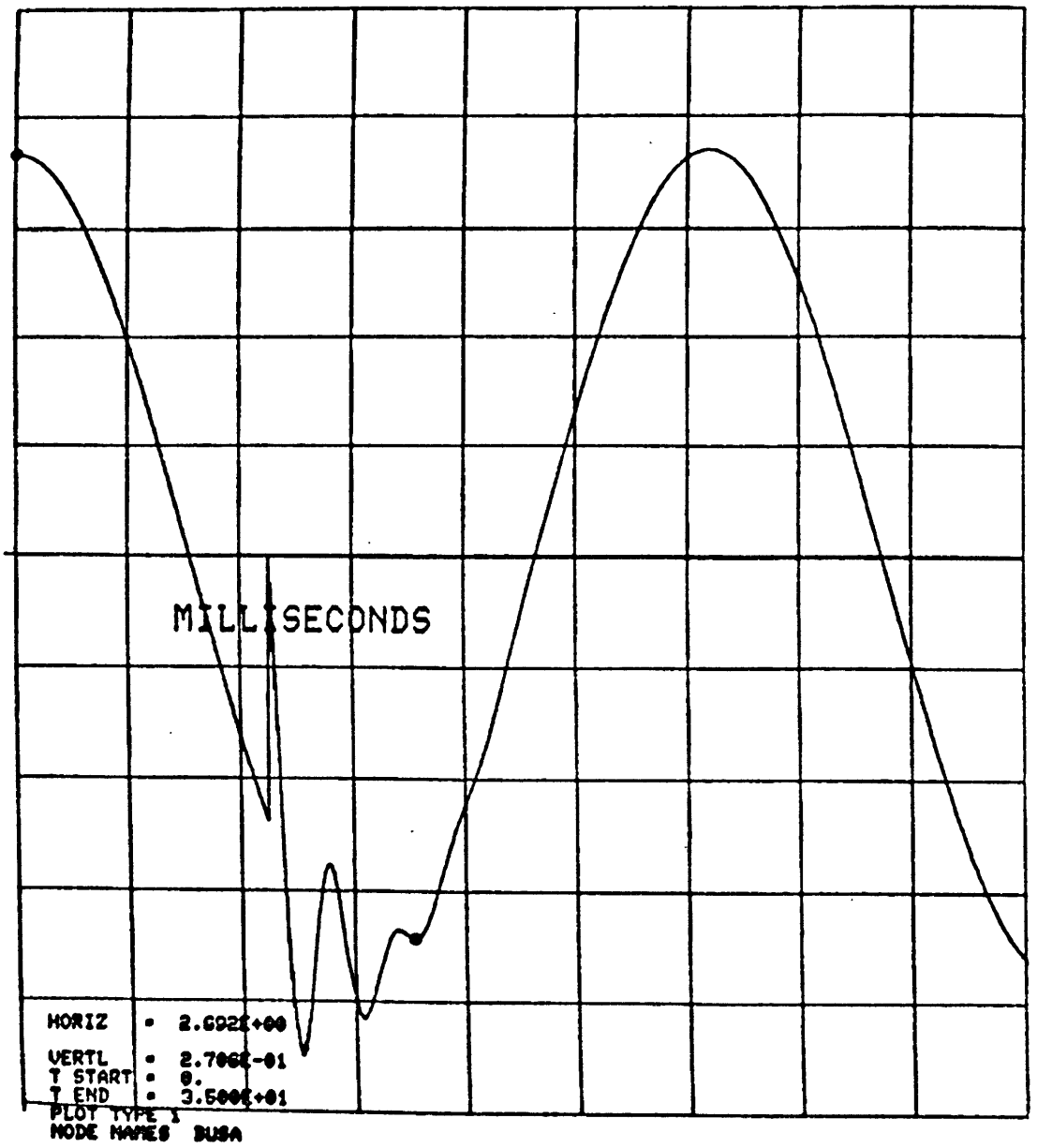

Figure 30 Computer plot of the bus voltage as a function of time for the "single bank" case. Energization 2.0 ms from voltage zero.

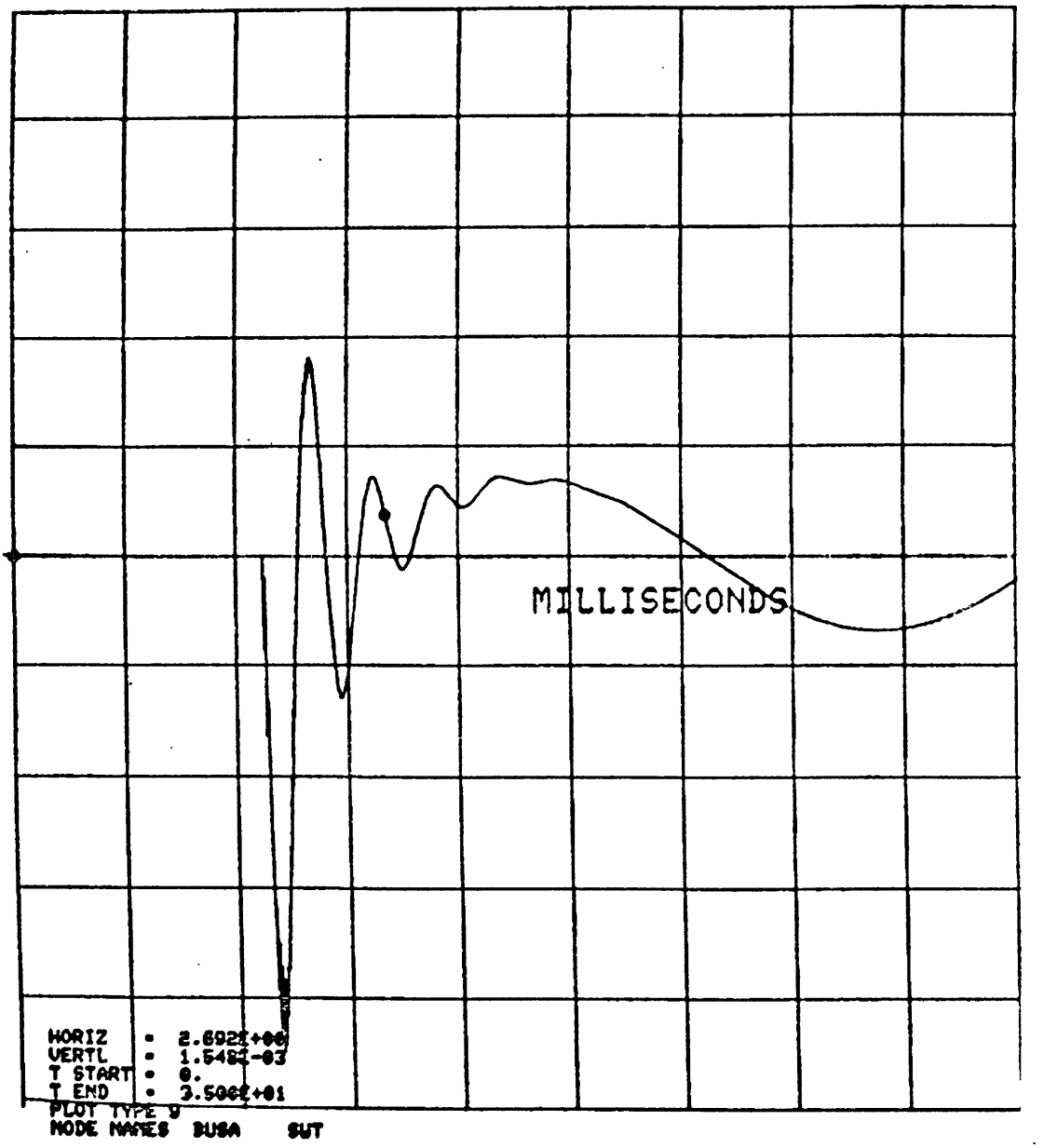

Figure 31 Computer plot of the capacitor current as a function of time for the "single bank" case. Energization 2.0 ms from voltage zero.

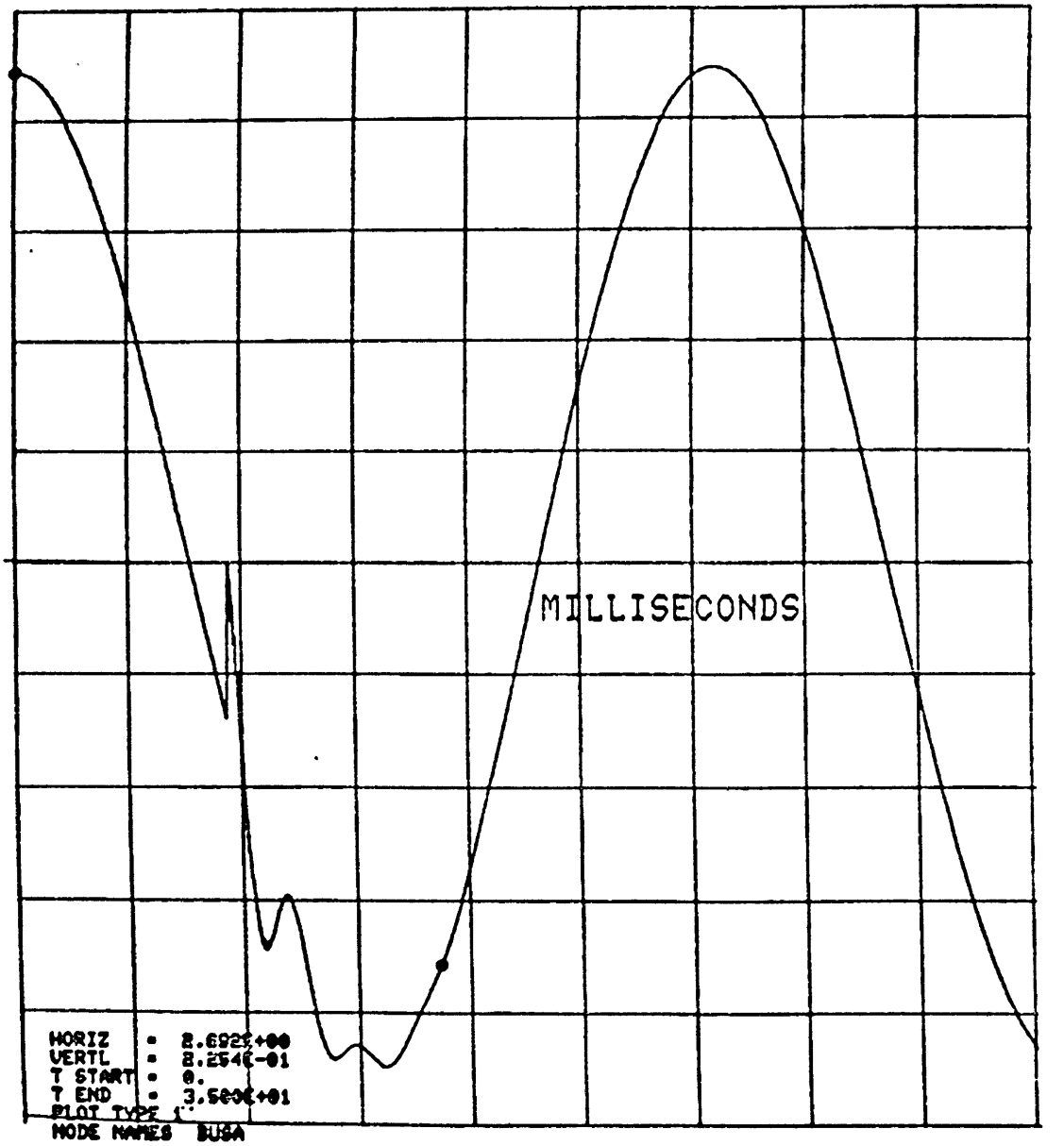

Figure 32 Computer plot of the bus voltage as a function of time for the "single bank" case. Energization 1.0 ms from voltage zero.

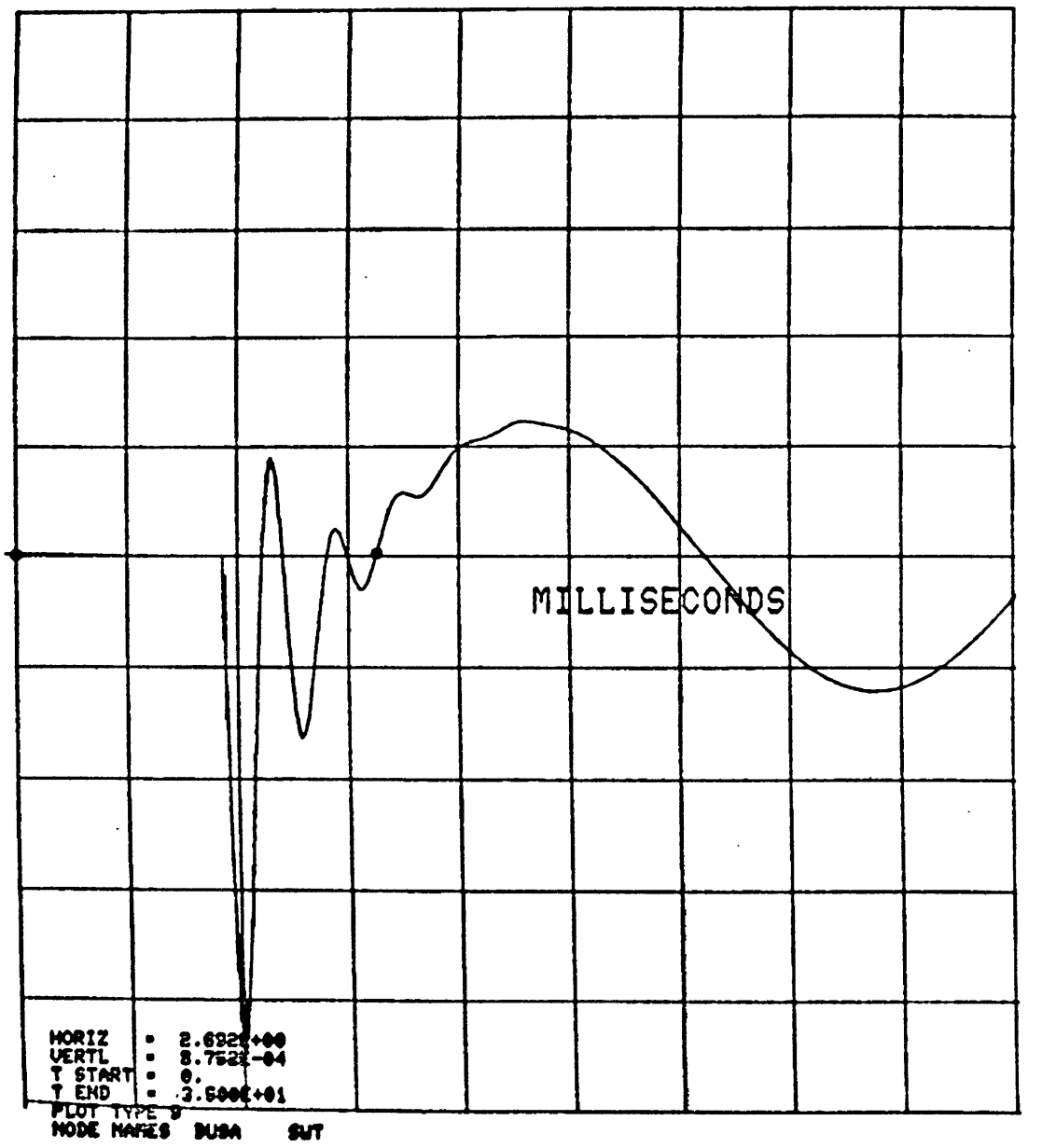

Figure 33 Computer plot of the capacitor current as a function of time for the "single bank" case. Energization 1.0 ms from voltage zero.

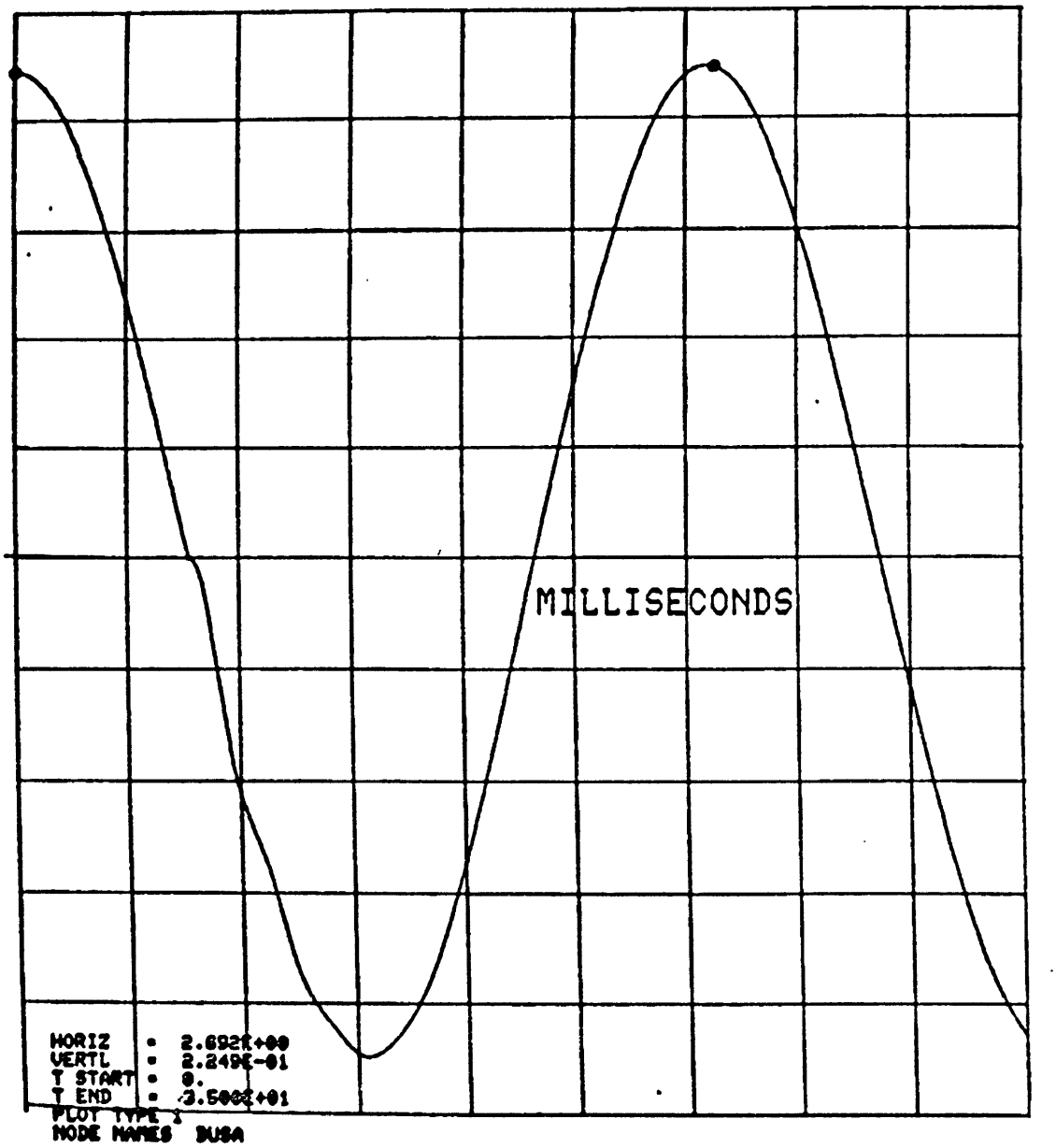

Figure 34 Computer plot of the bus voltage as a function of time for the "single bank" case. Energization at voltage zero.

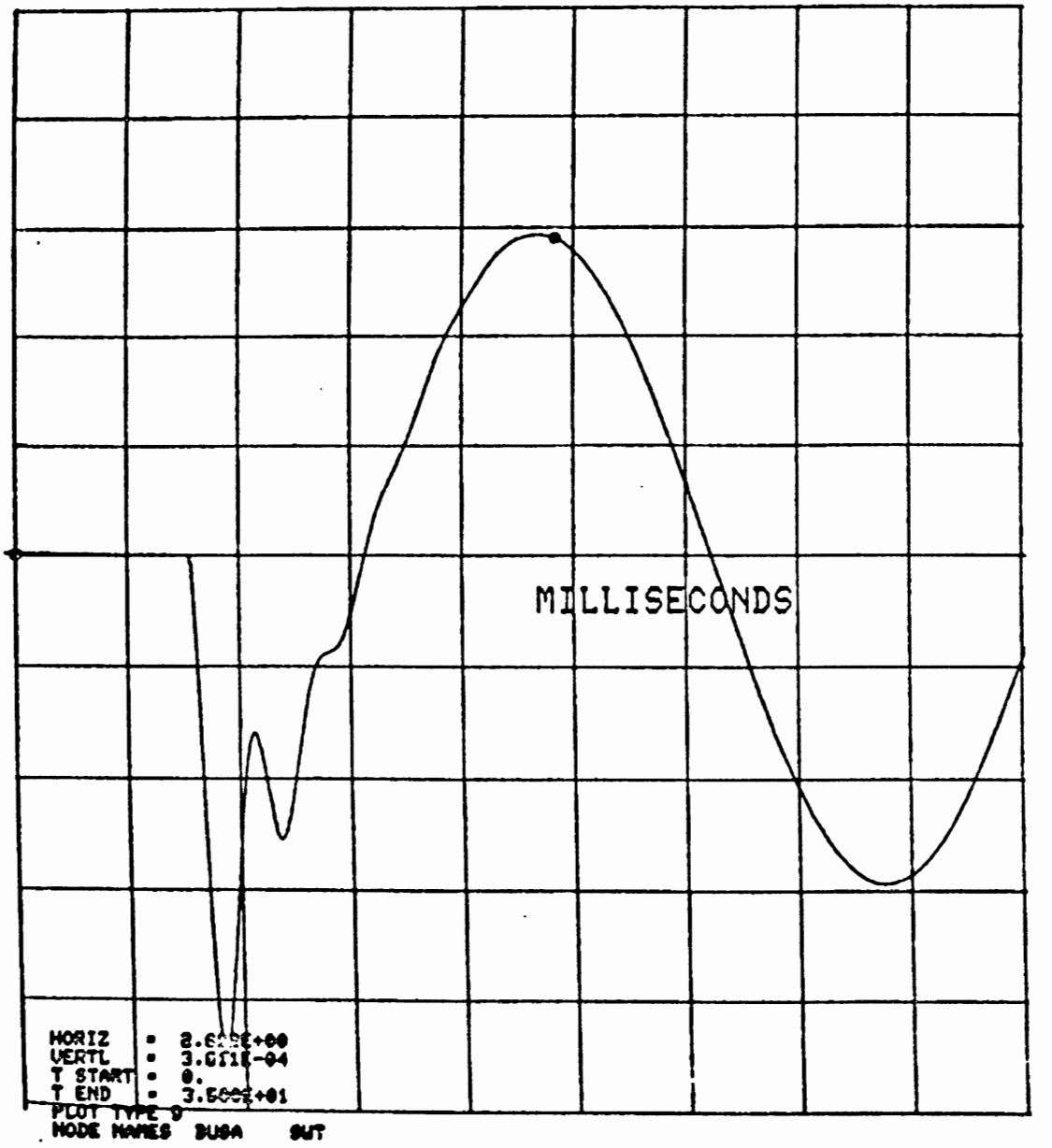

Figure 35 Computer plot of the capacitor current as a function of time for the "single bank" case. Energization at voltage zero.

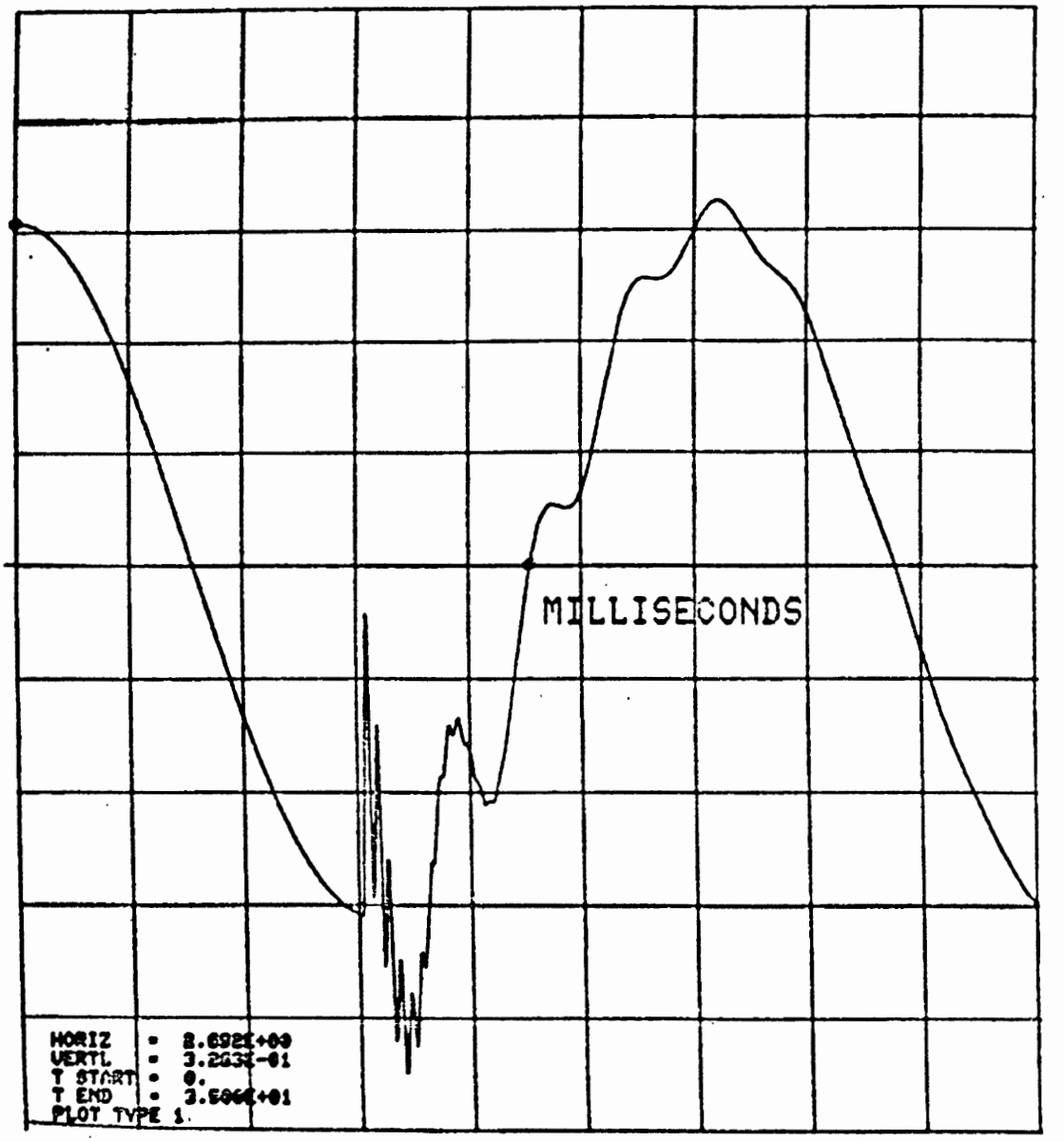

Figure 36 Computer plot of the bus voltage as a function of time for the "back to back" case. Energization 4.17 ms from voltage zero.

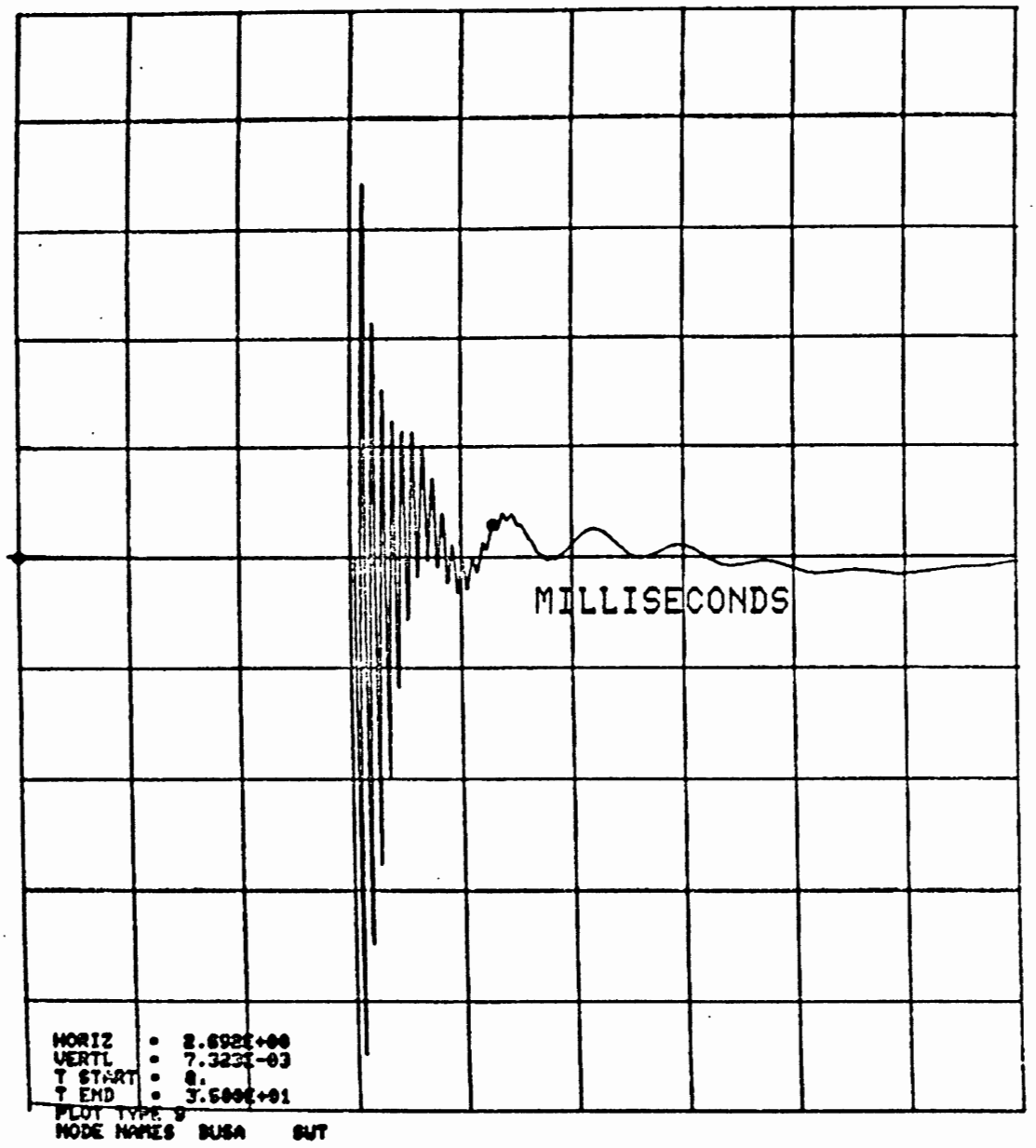

Figure 37 Computer plot of the capacitor current as a function of time for the "back to back" case. Energization 4.17 ms from voltage zero.

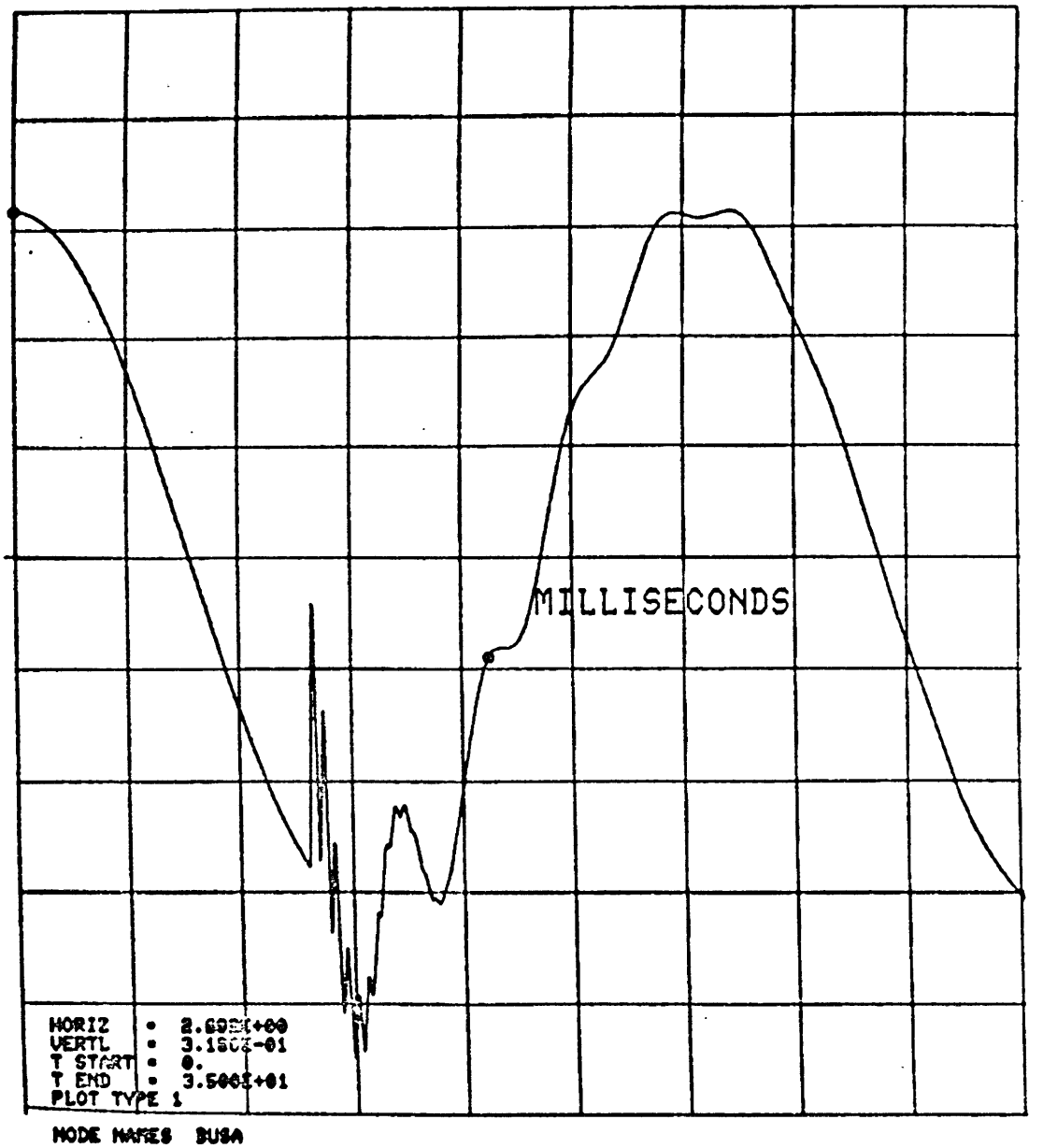

Figure 38 Computer plot of the bus voltage as a function of time for the "back to back" case. Energization 3.0 ms from voltage zero.

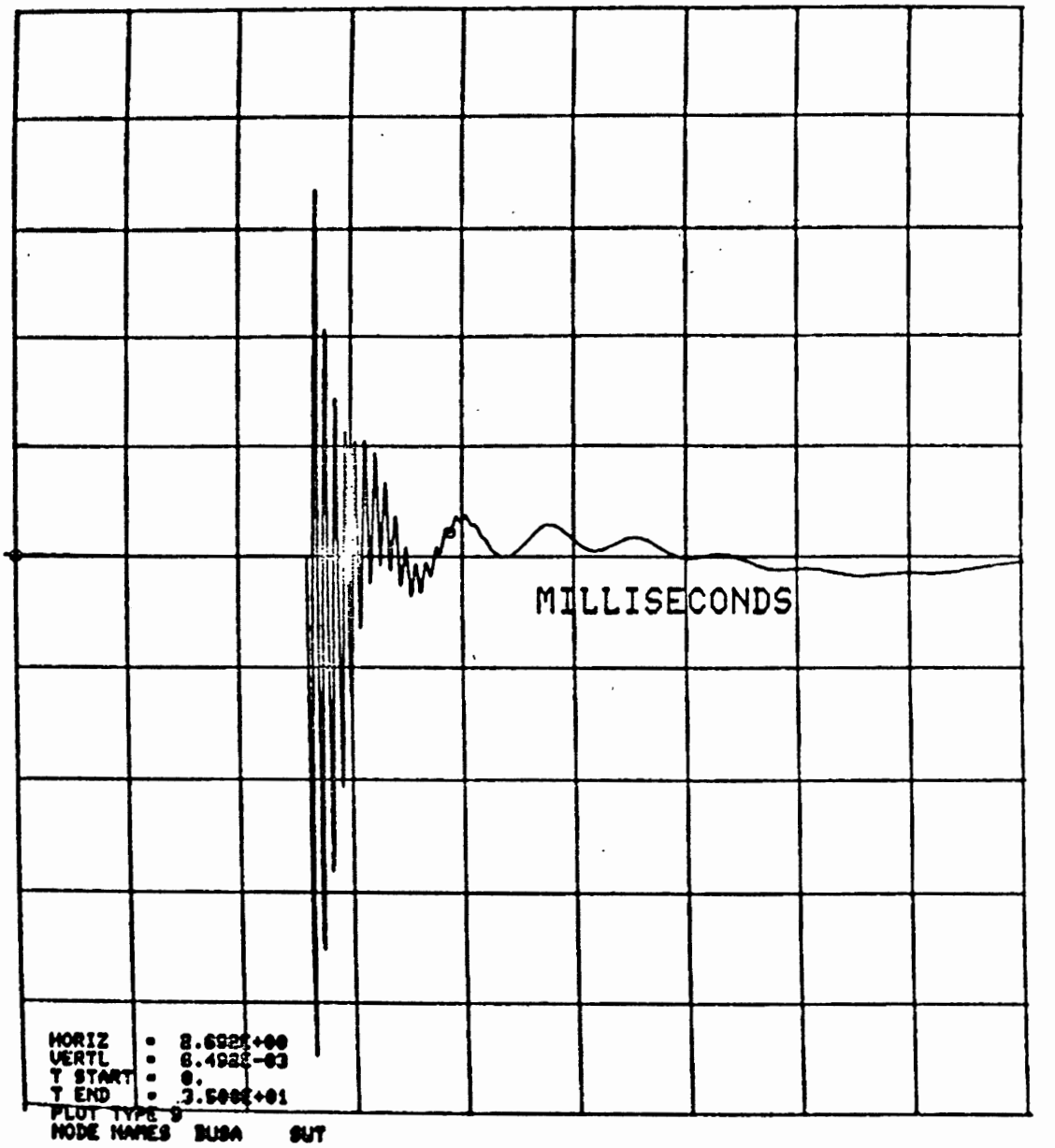

Figure 39 Computer plot of the capacitor current as a function of time for the "back to back" case. Energization 3.0 ms from voltage zero.

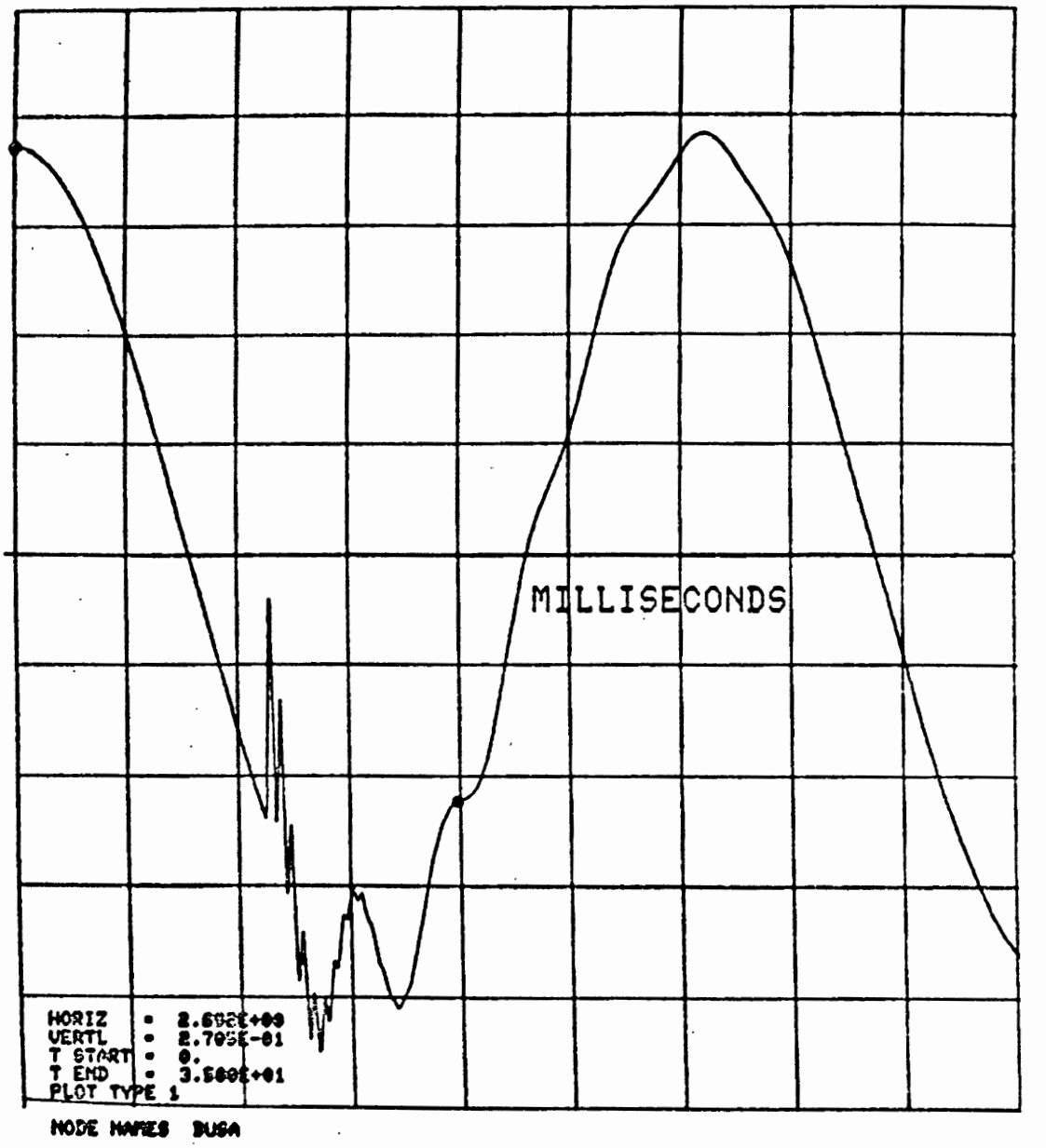

Figure 40 Computer plot of the bus voltage as a function of time for the "back to back" case. Energization 2.0 ms from voltage zero.

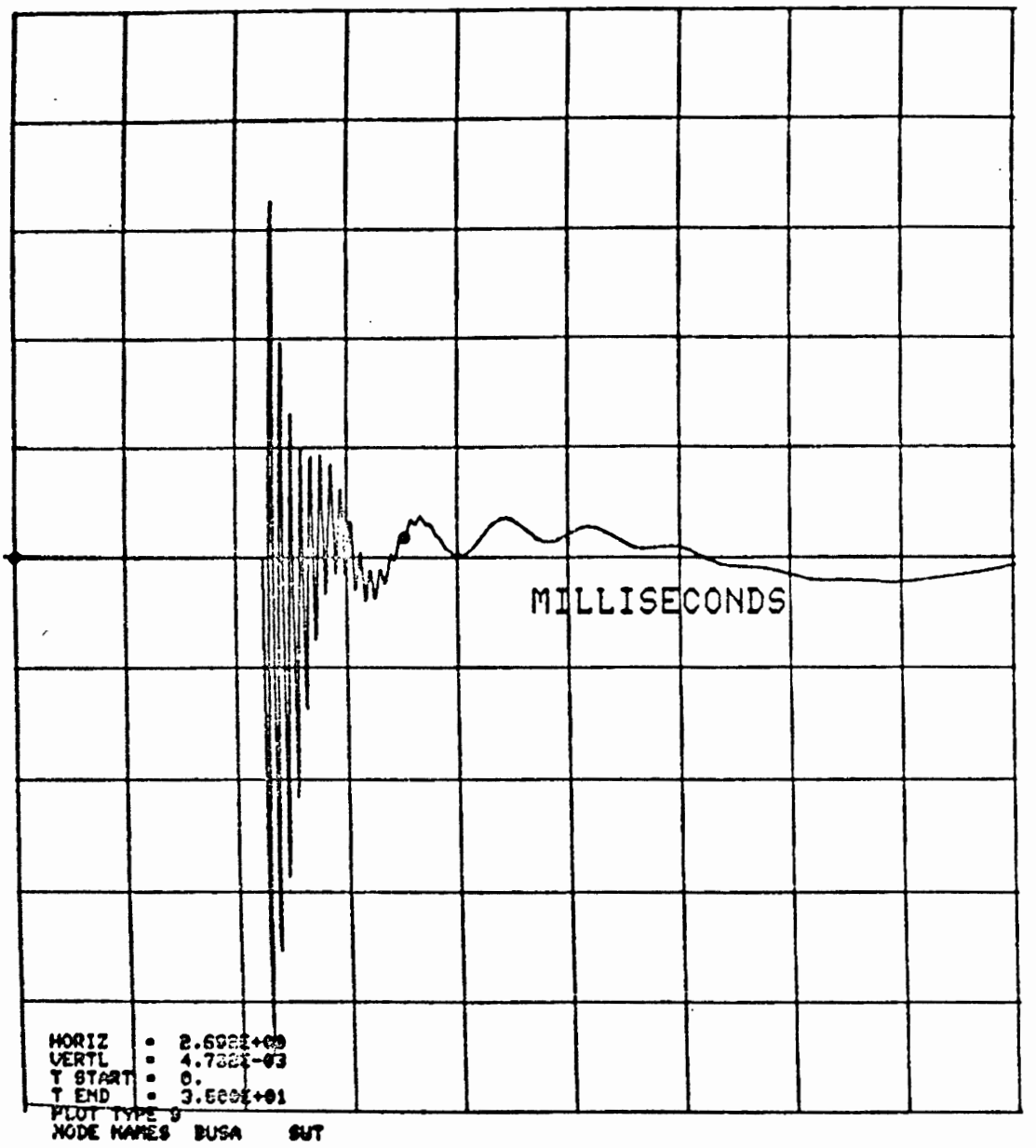

Figure 41 Computer plot of the capacitor current as a function of time for the "back to back" case. Energization 2.0 ms from voltage zero.

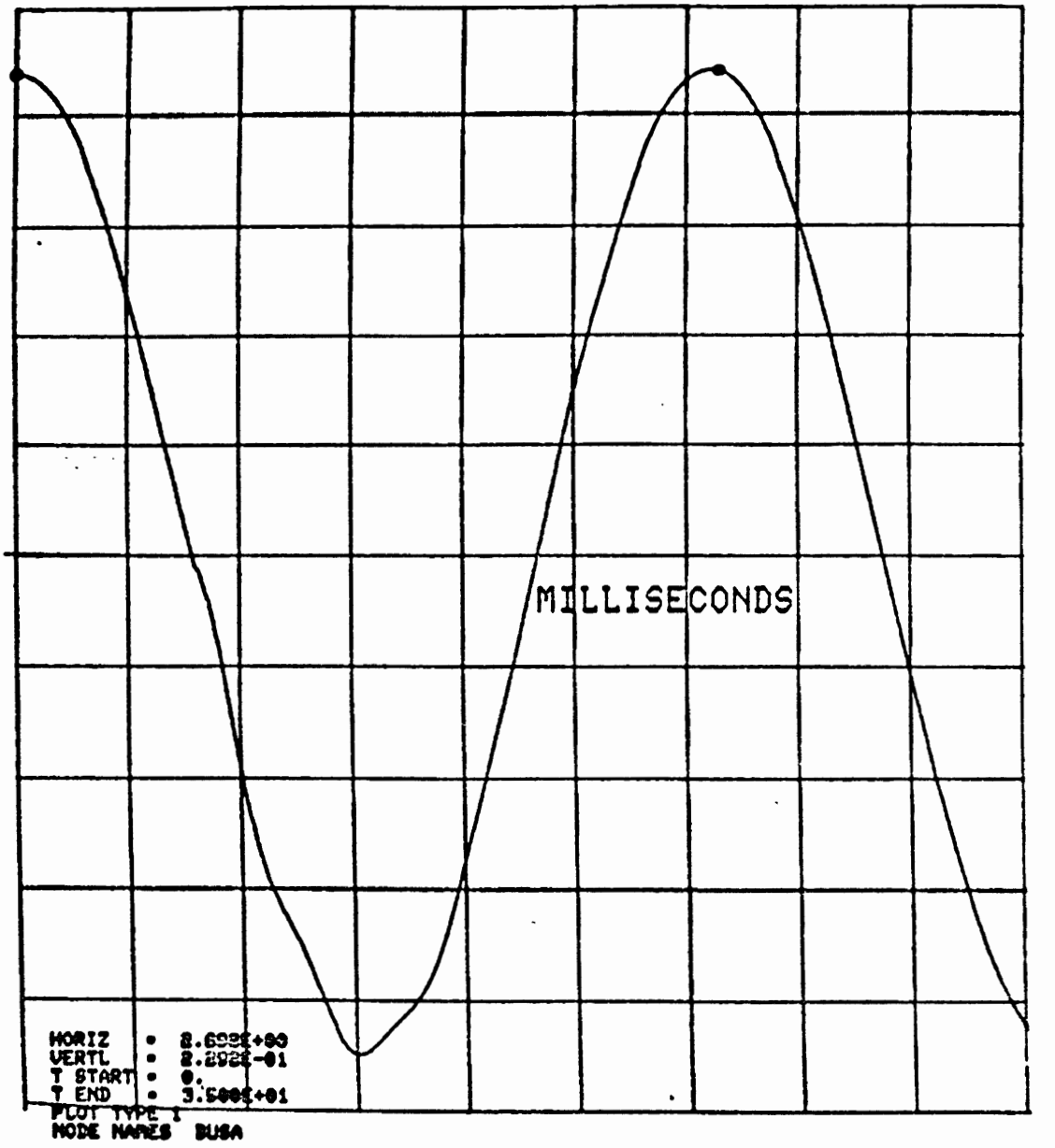

Figure 42 Computer plot of the bus voltage as a function of time for the "back to back" case. Energization at voltage zero.

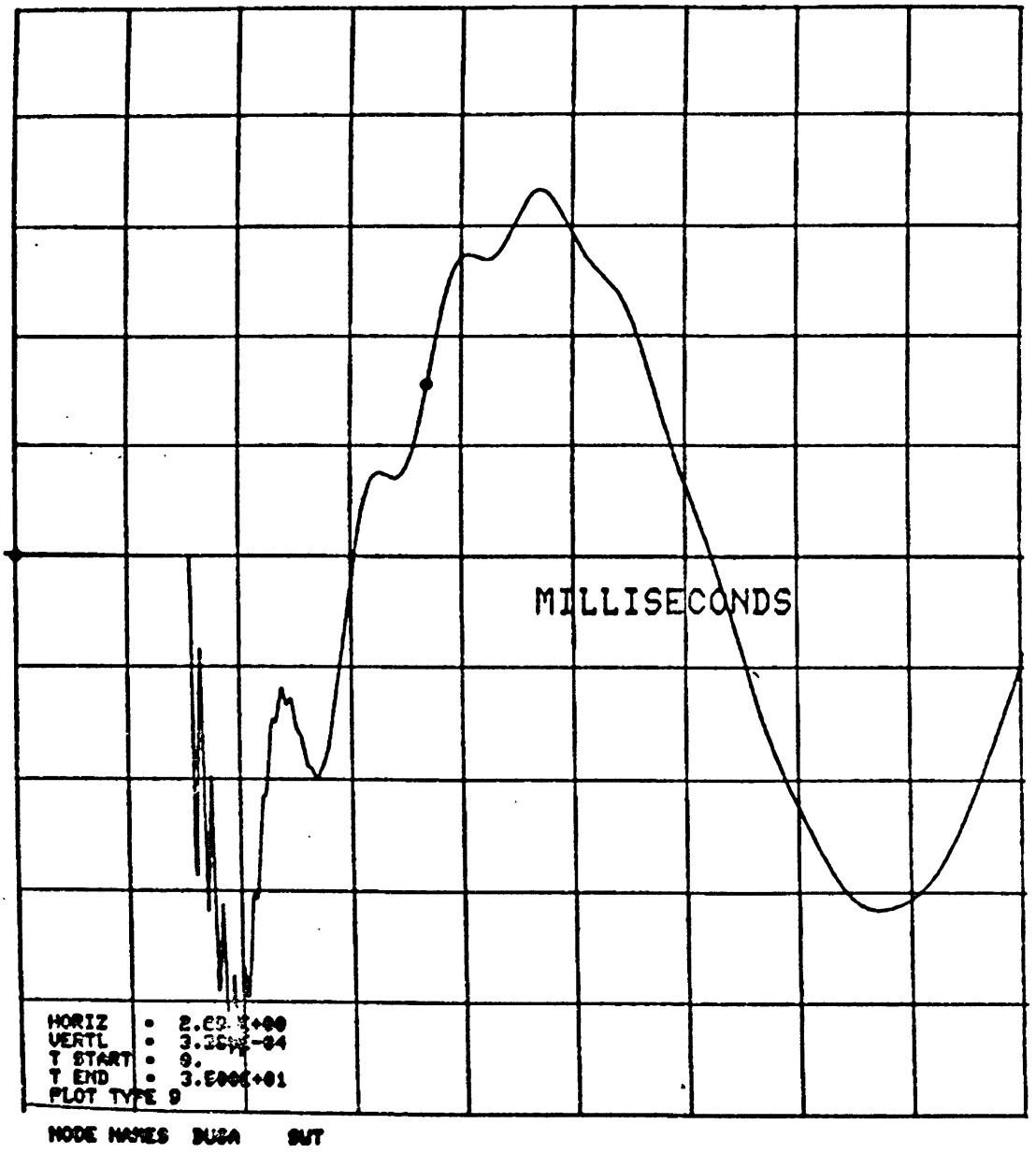

Figure 43 Computer plot of the capacitor current as a function of time for the "back to back" case. Energization at voltage zero.

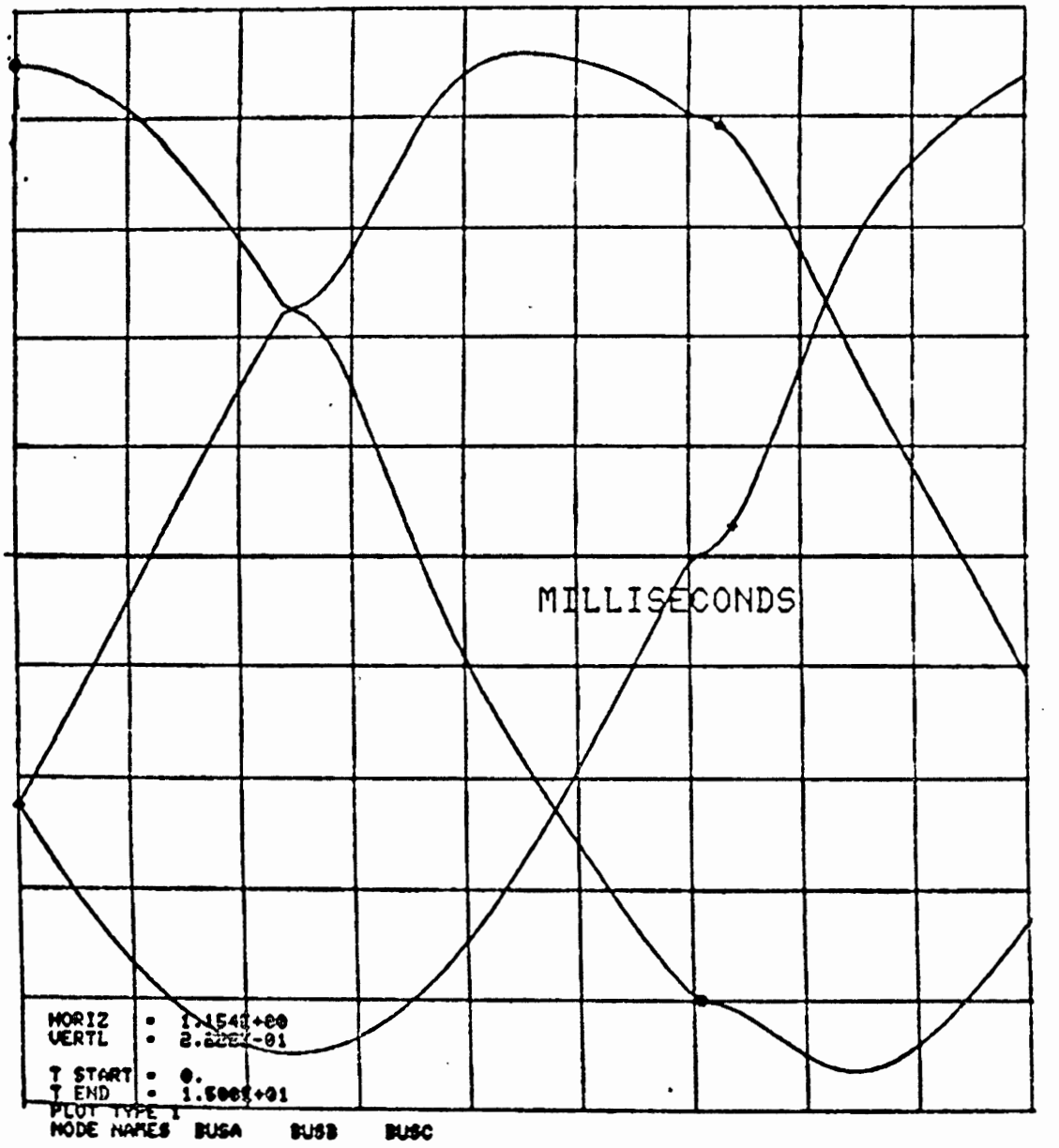

Figure 44 Computer plot of the three-phase bus voltages as a function of time for a "single bank" delta connected configuration. Energization was not at voltage zero, but when the voltage across each leg was minimum.

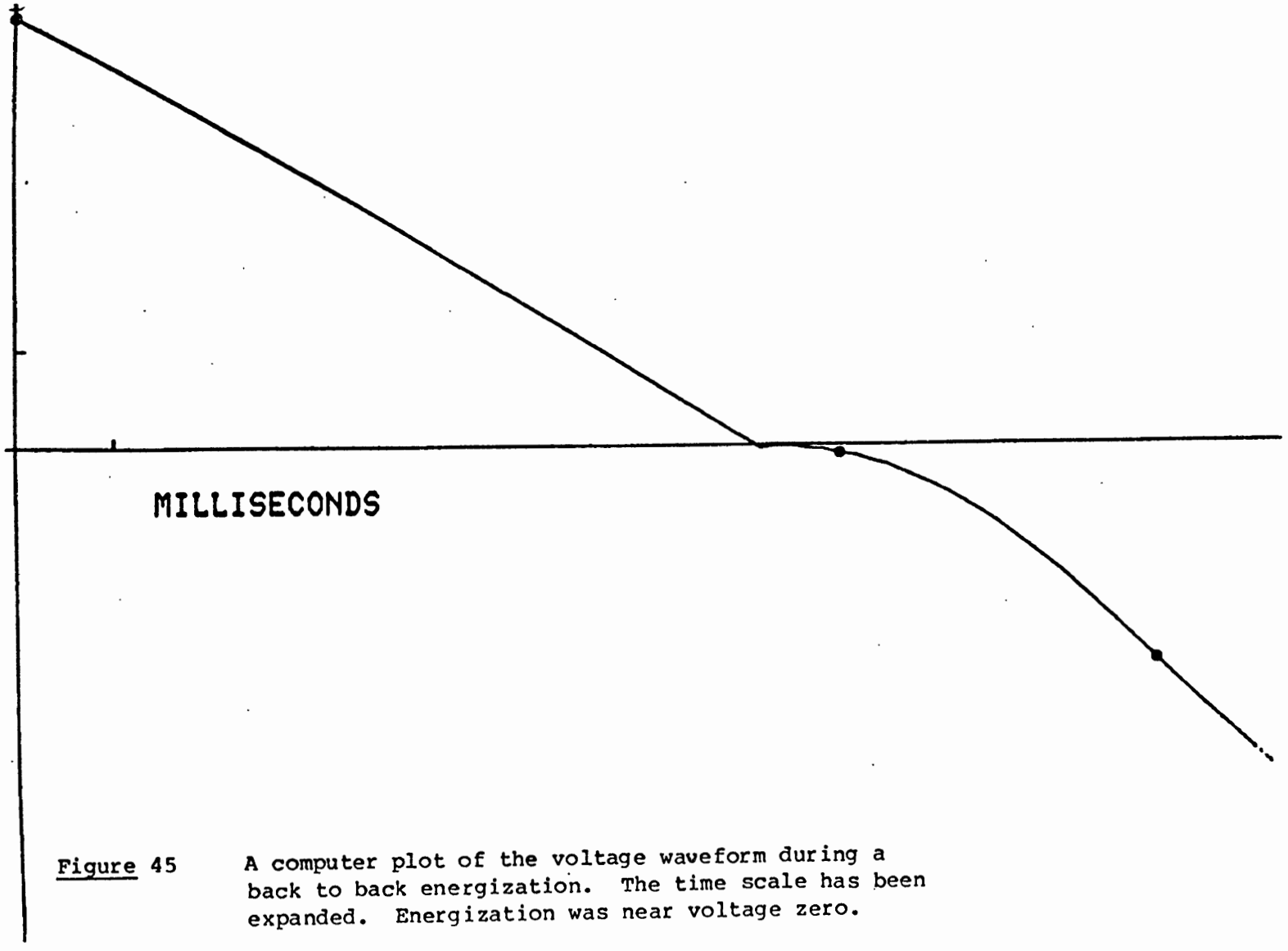

Figure 45 A computer plot of the voltage waveform during a back to back energization. The time scale has been expanded. Energization was near voltage zero.

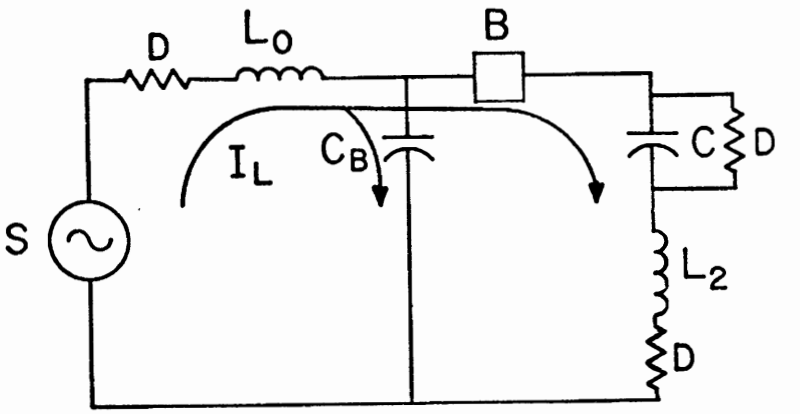

Figure 46 The model used for the computer analysis. Damping (linear) has been included.

APPENDIX II

THE VACUUM BREAKER THERMAL EFFECTS AND MODIFICATIONS

The vacuum breaker's ability to operate within +/- 1.0 ms over the temperature range normally expected in an unprotected substation is crutial to the success of the zero-voltage closing technique. The solenoid may well be the critical component limiting the temperature response of the system. With this in mind a model of the solenoid was developed for analysis. Reliable parameters for the model were never found and the long term test provided emperical results which indicated that temperature was not a severe problem. Although the model was not used, it is included so that it may be tried if the necessary parameters do become more readily available.

An attempt was made to analyze the effects of thermal changes on the vacuum breaker closing time. The analysis examined the effects of temperature induced changes in the capacitance value of the energy storage capacitors and its effect on closing time. The model used is shown in Figure 47. An equation for the total reluctance can be written(24,25):

$$R = \frac{g}{2 a u_o} \left(\frac{1}{h} + \frac{1}{x} \right)$$

$$L = \frac{2 u_o a h}{g} \left(\frac{x}{h+x} \right)$$

From this the value of inductance found.

$$L = N^2 \frac{1}{R}$$

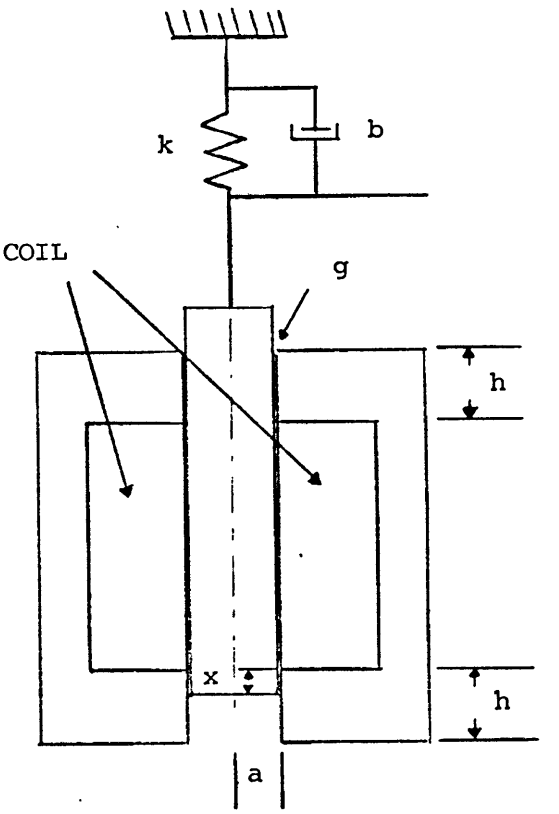

Figure 47 A solenoid model, used to represent the closing mechanism of the vacuum breaker(23).

$$L = \frac{2\,u_o ah}{g} \quad \frac{x}{h+x}$$

The force on the solenoid can then be calculated:

$$F = \frac{JW}{Jx} \quad , \quad w = \frac{1}{2}Li^2$$

$$F = \frac{1}{2}i^2 \frac{dl}{dx}$$

$$F = \frac{2\,u_o ah}{g} \quad \frac{hi^2}{(h+x)^2}$$

The counter emf is:

$$e = \frac{d}{dt}(Li) = \frac{Ldi}{dt} \quad \frac{idL}{dx} \quad \frac{dx}{dt}$$

We can now write two equations to describe the system.

The force equation:

$$\frac{2\,u_o ah}{g} \quad \frac{hi^2}{2} = M\frac{d^2x}{2} + b\frac{dx}{dt} + K(l_o - x)$$

And the electric circuit equation:

$$ri + \frac{2\,u_o ah}{g} \quad \frac{x}{n+x} \quad \frac{di}{dt} \quad \frac{2\,u_o ah}{g} \quad \frac{hi}{(h+x)^2} \quad \frac{dx}{dt} \quad \frac{1}{c} \quad idt + V_o = 0$$

These equations might be solved by numerical techniques. In attempting to obtain numerical values from the manufacturer, I found that they were not available. Measuring them was considered, but in

discussion with the manufacturer I found that their testing had demonstrated that thermal expansion of mechanical parts would because for more timing deviation than electrical parameter changes. It was therefore determined not to analyze this any further. Thermal/ mechanical analysis was also impractical because material characteristics were not available, so thermal effects were evaluated during prototype evaluation.

The control circuitry of the vacuum breaker was modified to improve closing time accuracy. The changes included, (1) a voltage regulator to charge and maintain the voltage of the energy storage capacitors; and (2) an SCR in series with each close solenoid. Figure 49 shows a simplified control circuit of a single pole before modification and Figure 50 shows a simplified control circuit after modification.

The circuit diagram of the voltage regulator is shown in Figure 50. The circuit diagram, a single phase of the interface unit, is shown in Figure 51.

The device that is used to control the vacuum breaker was developed by BPA for use on 500 kV power circuit breakers to control switching surges. A block diagram is shown in Figure 52. It basically uses a zero crossing detector to generate timing pulses. An adjustable delay circuit allows the output signal to be adjusted in relation to the synchronizing 60 Hertz source, in this case, the A phase bus voltage.

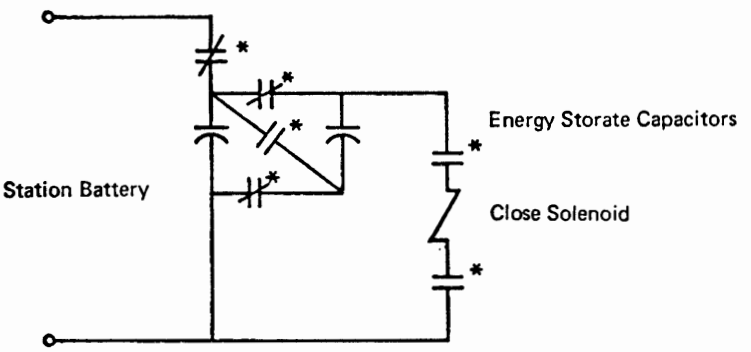

*CONTACT ON CLOSE CONTACTOR

Figure 48 The simplified control circuit of the vacuum breaker before modifications.

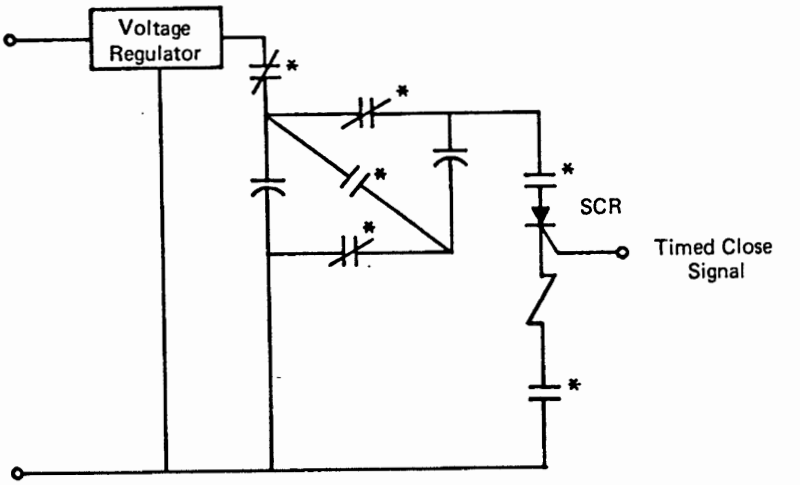

*CONTACT ON CLOSE CONTACTOR

Figure 49 The simplified control circuit of the vacuum breaker after modifications.

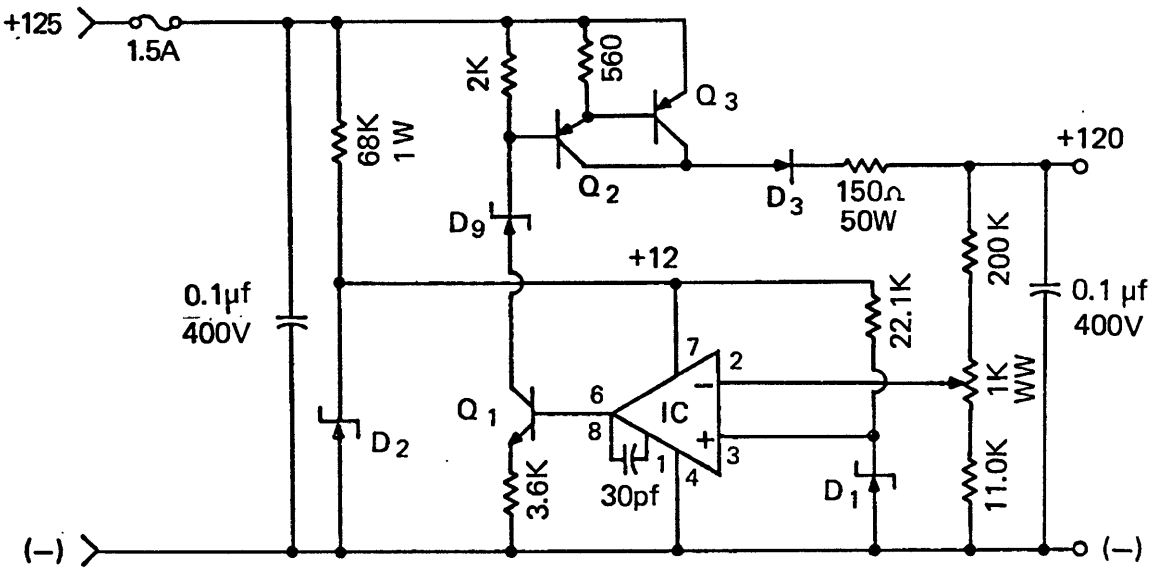

Standby current ≈ 2.9 ma

D_9 = 82V, 10%, 400mW IN983A
D_1 = 6.4V, 5%, 0.25ma PS1313A
D_2 = IN963B, 12V, 5%
D_3 = 400 PIV, 3A.
IC = LM108/LM208H
Q_1 = JAN 2N3439, 300V
Q_2,Q_3 2N6212, 300V, PNP

Figure 50 The circuit diagram of the voltage regulator that was added to the vacuum breaker.

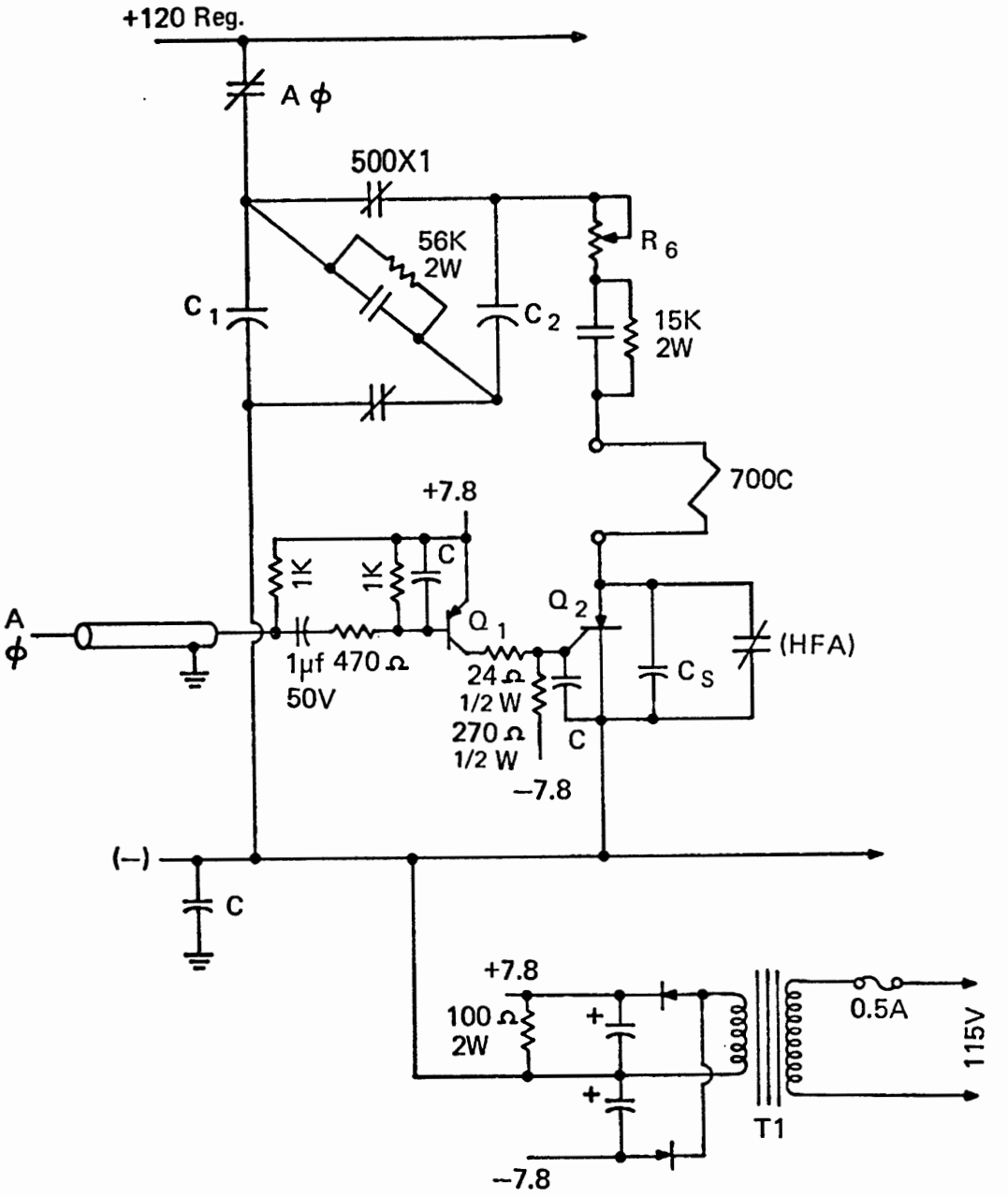

Figure 51 The circuit diagram of the interface circuit. This circuit connected the vacuum breaker to the control device.

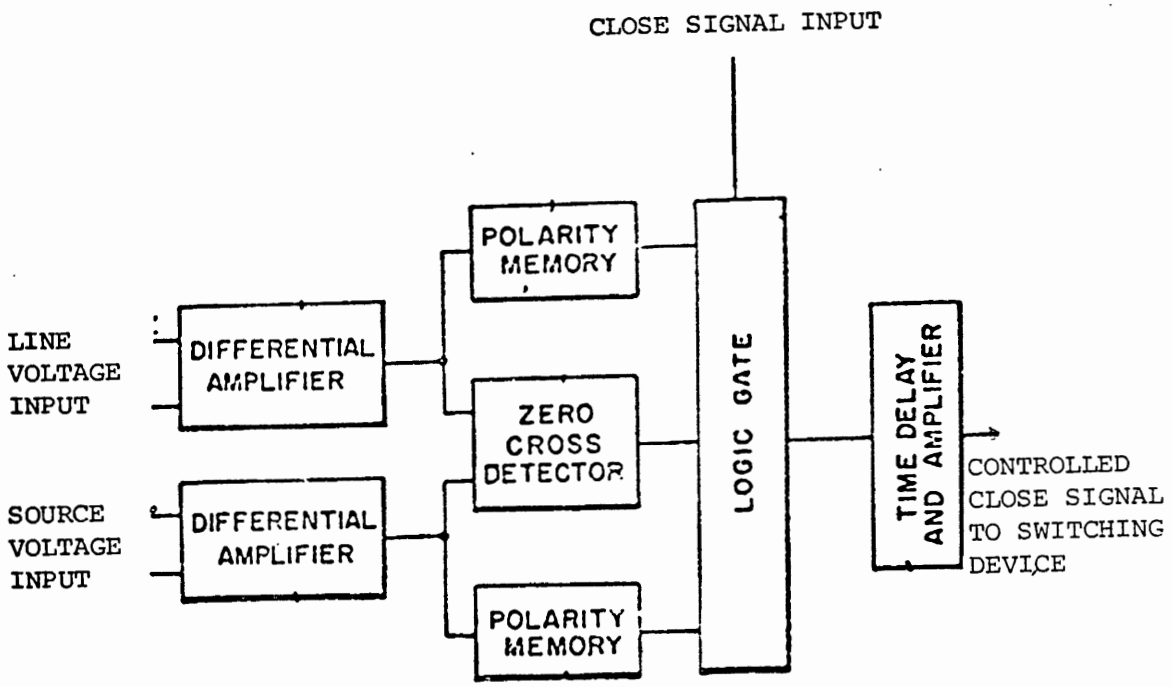

Figure 52 Block diagram of the BPA Controlled Closing Device which was used to control the vacuum breaker.

APPENDIX III

FIELD TEST

The high magnitude, high frequency electromagnetic environment that occurs in a substation during a transient event makes accurate measurement difficult. Special procedures and practices are employed to increase the accuracy of transient measurements possible.

BPA uses a 40 foot van to house and shield instruments during field tests. The trailer was positioned slightly closer to the capacitor yard than was desirable due to physical constraints. It was, however, off the peninsula grounding grid.

Electrical power for the instruments was obtained from an engine-generator positioned close to the van. Station service outlets were available but their ground source was almost 600 feet away. A "ground loop" this long could effect measurements or result in a flashover in the station service wiring. Connection to the generator was made through a 25 kVA isolation transformer. Individual isolation transformers were provided for each instrument in the trailer as well.

The vacuum breaker obtained its operating power from a portable station battery to avoid any grounding problem.

Haefely wideband voltage dividers were placed on the bus side of the bank protection breaker. They have a frequency response from DC to 10 MHz. These dividers were choosen because of their high frequency response and because their low capacitance (100 pF) would have little effect on the bus capacitance and would not disturb the circuits being measured.

Coupling capacitor dividers were installed across the capacitor bank to measure voltage. They were choosen due to physical size restrictions in the location they were placed. Their large capacitance (2,500 pF) will have little effect in parallel with the capacitor bank.

Current transformers were placed on each leg of the neutral and a coaxial shunt was placed on A phase neutral(25). The signal from the shunt could not be connected directly to our instruments as it is connected directly to the neutral where a high transient potential exists. A second trailer was placed near the neutral and records made on an oscilloscope with a camera. The shunt was important as the current transformers' frequency response was not known.

The most important considerations are shielding and grounding(26). The instrument cables were all triaxial (double shielded) and were placed inside of a conduit. The triaxial cable performs as a neutralizing transformer when properly connected. The cables were laid out to form a radial system(14).

The radial system has only one ground point, where the capacitor yard ground mat connects to the main station ground mat. This reduces errors due to ground loops.

Signals were recorded on (1) oscillographs to provide immediate results, and (2) an analog tape recorder to provide high frequency response (DC to 40 KHz.) and for a permanent record.

The A-phase bus voltage was recorded on a digital transient recorder. This allowed high frequency response and pre-event information to be recorded. Figures 14, 15, 16, 17, 18, and 19 were recorded on the digital transient recorder.

Peaking reading voltmeters were used to record fence to neutral potentials, control cable potentials, step potentials and touch potentials(27). Step and touch potentials are also known as personnel intercept potentials as they are potentials between ground points, and between ground points and objects that personnel might come in contact with.

TABLE I

TEST DATA - SINGLE BANK SWITCHING

Operation	Peak Current	Fence to Neutral Potential	Fence Touch Potential
Load Break Switch with Resistors	392 A	3.0 kV	282 V
Load Break Switch without Resistors	735 A	4.5 kV	292 V
Vacuum Breaker @ voltage zero	880 A	10.3 kV	100 V
Vacuum Breaker @ voltage zero	637 A	1.2 kV	6 V
Vacuum Breaker @ voltage zero	390 A	1.2 kV	0 V
Vacuum Breaker +1.0 ms	1.2 kA	2.6 kV	90 V
Vacuum Breker +2.0 ms	1.6 kA	3.4 kV	184 V
Vacuum Breaker +4.0 ms	1.6 kA	4.6 kV	364 V

TABLE II

TEST DATA - BACK TO BACK SWITCHING

Operation	Peak Current	Fence to Neutral Potential	Fence Touch Potential
Load Break Switch with Resistors	2.6 kA	No record	180 V
Load Break Switch without Resistors	24.5 kA	13.5 kV	912 V
Vacuum Breaker @ voltage zero	2.94 kA	2.0 kV	88 V
Vacuum Breaker @ voltage zero	2.45 kA	1.8 kV	84 V
Vacuum Breaker @ voltage zero	163 A	800 kV	6 V
Vacuum Breaker +1.0 ms	6.85 kA	4.5 kV	284 V
Vacuum Breker +2.0 ms	12.7 kA	No record	584 V
Vacuum Breaker +4.0 ms	19.6 kA	12.8 kV	848 V